Geomorphology 495 (2026) 110131



Contents lists available at ScienceDirect

Geomorphology

journal homepage: www.journals.elsevier.com/geomorphology



# Effects of sediment connectivity changes on channel evolutionary trajectory: the case study of the Taro and Ceno rivers in the Northern Apennines (Italy)☆

Sharon Pittau [a], Vittoria Scorpio [a,b,*]

[a] CRICT—Inter-Departmental Research and Innovation Centre on Constructions and Environmental Services, University of Modena and Reggio Emilia, Modena, Italy
[b] Department of Chemical and Geological Sciences, University of Modena and Reggio Emilia, Modena, Italy

ARTICLE INFO

*Keywords:*
Active channel changes
Bed level incision
Afforestation
Connectivity index
Gravel mining
Northern Apennines

ABSTRACT

The post-1950s evolutionary trajectories of the Taro and Ceno rivers (Northern Apennines, Italy) were investigated, focusing on the correlation between channel adjustments and sediment alterations. The specific aims were to: i) highlight similarities and dissimilarities between the evolutionary trajectories of the two rivers; ii) assess the role of sediment connectivity decrease caused by land use changes along the hillslopes, and iii) evaluate the impact of gravel mining.

Changes in active channel width and bed level were quantified using multi-temporal orthophotos (1954–2020) and topographical cross-sections. Land use dynamics were reconstructed through multi-temporal land cover maps, and changes in structural sediment connectivity were assessed by applying the Index of Connectivity (IC). Evolution of landslide-prone areas was analysed to estimate changes in sediment supply, and the influence of anthropogenic activities was also considered through mapping gravel mining areas and in-channel works.

Results showed progressive afforestation, after the 1950s in the Ceno and after the 1970s in the Taro basin, with decreases in landslide-prone areas and IC. Hillslope stabilization caused a decrease in sediment supply to both channels, with subsequent channel narrowing and bed incision (−50 % and −3.3 m in the Taro and −38 % and −2.5 m in the Ceno, respectively). More intense morphological changes in the Taro, especially between 1954 and 1976, were linked to the intense gravel mining activity, completely absent along the Ceno. The combined effects of catchment-scale afforestation and reach-scale gravel extraction therefore played a key role in shaping the dissimilarities in the evolutionary trajectories between the two rivers.

## 1. Introduction

River's morphology and dynamics are driven by the inputs of water and sediment and by the degree of sediment transfer through the channel system (Thorne, 1997; Bracken et al., 2015; Heckmann et al., 2018; Wohl et al., 2019). The potential of sediments to be mobilized within a geomorphic system is defined as sediment connectivity (Borselli et al., 2008; Cavalli et al., 2013; Poeppl et al., 2017; Heckmann et al., 2018; Najafi et al., 2021). The amount of sediment supply from hillslopes (i.e., landslides, debris flows, badlands) to the river is significantly influenced by the degree of coupling between source areas and the fluvial system (Cavalli et al., 2019; Koreňová et al., 2024; Pitscheider et al., 2024). More generally, the extent to which landscape units are contiguous or physically linked to one another is explained by the concept of structural connectivity (Tischendorf and Fahrig, 2000; Wainwright et al., 2011; Cavalli et al., 2017). Structural connectivity is very sensitive to the presence of natural impediments – such as pediment areas, alluvial fans, plains - and anthropogenic barriers such as weirs, check-dams and dams (Fryirs et al., 2007; Cavalli et al., 2013; Poeppl et al., 2020).

Connected sediment sources can significantly impact river sediment balance and morphodynamics, as high rates of sediment are supplied to the rivers, whereby processes such as bed level aggradation and active channel widening are promoted and complex and dynamic channel morphologies (e.g. multi-thread or transitional channels) are usually observed (Reid and Dunne, 1996; Hassan et al., 2005; Scorpio et al.,

☆ This article is part of a Special issue entitled: 'Denudation dynamics' published in Geomorphology.

* Corresponding author at: Department of Chemical and Geological Sciences, University of Modena and Reggio Emilia, via Campi 103, 41125, Modena, Italy.
*E-mail addresses:* sharon.pittau@unimore.it (S. Pittau), vittoria.scorpio@unimore.it (V. Scorpio).

https://doi.org/10.1016/j.geomorph.2025.110131
Received 1 August 2025; Received in revised form 5 December 2025; Accepted 6 December 2025
Available online 8 December 2025
0169-555X/© 2025 The Authors. Published by Elsevier B.V. This is an open access article under the CC BY-NC-ND license (http://creativecommons.org/licenses/by-nc-nd/4.0/).

2022). In contrast, when sediment sources remain disconnected from the channel network, their contribution to river sediment budget is minimized and channels can become deficient in bars or undergo active channel incision and narrowing (Brenna et al., 2021; Piasecka et al., 2025; Vergari et al., 2025).

Human pressures, acting at both catchment and reach scales, had a significant impact on sediment conveyance and natural dynamics of river systems, particularly in developed countries over the last decades (Hooke, 2006; Wohl, 2006, 2020; Downs and Piégay, 2019; Stecca et al., 2019; Scorpio et al., 2024b). At the global scale, Dethier et al. (2022) documented that dam construction in the northern hemisphere has reduced global sediment transport from rivers to oceans by 49 % compared to pre-dam conditions. In contrast, in the southern hemisphere, sediment transport has increased in 36 % of the analysed rivers due to land-use changes associated with deforestation.

Indirect pressures related to land use changes in the catchments, such as afforestation or deforestation, agricultural expansion or farmland abandonment, have modified transverse (slope-to-river) connectivity, influencing sediment delivery from hillslopes and regulating the extent of sediments available to the fluvial system (Blanton and Marcus, 2009; Koreňová et al., 2024; Piasecka et al., 2025). In many European rivers, upland afforestation due to depopulation of mountain areas and farmland abandonment, led to hillslopes stabilization and a decrease in sediment connectivity (Persichillo et al., 2018; Llena et al., 2019, 2024), resulting in a deficit in sediment propagation downstream and channel degradation (Fryirs and Brierley, 2001; Lach and Wyżga, 2002; Liébault and Piégay, 2002; Liébault et al., 2005; García-Ruiz et al., 2010; Buendia et al., 2016; Llena et al., 2020; Scorpio and Piégay, 2021).

Direct human sediment alteration in the fluvial system, including the construction of dams and other transverse works, and in-channel gravel mining, disrupted longitudinal sediment connectivity by trapping sediments with detrimental effects on channel morphology (Kondolf, 1997; Batalla et al., 2004; Zawiejska and Wyżga, 2010; Rollet et al., 2014; De Vincenzo et al., 2017; Fortugno et al., 2017; Cucchiaro et al., 2019; Piasecka et al., 2025). Longitudinal structures prevented bank erosion, stabilized channel morphology and affected the lateral connectivity (Rinaldi and Simon, 1998; Davies et al., 2013; Scorpio et al., 2018; Marchi et al., 2019). In many rivers, gravel extraction altered the balance between sediment supply and transport capacity, resulting in channel narrowing, bed level incision and habitat loss (Kondolf, 1997; Rinaldi et al., 2005; Surian et al., 2009; Ziliani and Surian, 2012; Surian, 2022; Ferrer-Boix et al., 2023; Scorpio et al., 2024a). For example, Scorpio et al. (2024a) affirmed that the rapid channel changes observed in 15 rivers of the Eastern Italian Alps (upper Etsch River basin) from the 1950s to the 1990s, were mainly driven by the gravel mining carried out in the period 1970s–1990s. A cumulative volume of 6.1 million $m^3$ of gravel removed from the Etsch River channel network was estimated, that corresponded to about 150,000–200,000 $m^3$/year, which is a value from 3 to 5 times higher than the current coarse sediments transported by the Etsch River in the area (42,000 $m^3$/year).

The Taro River - located in the Northern Apennines in Italy - has undergone significant morphological alterations over the past decades (Clerici et al., 2015). The analysis of the Taro and its main tributary, the Ceno River, provides a representative case study to assess the impact of land use changes along the hillslopes and in-channel gravel mining on channel morphology. Many studies have analysed the relation between channel changes and controlling factors (see Scorpio et al., 2024b and references therein), most of them have highlighted the impact of in-channel human activities on sediment conveyance, but to the best of our knowledge, none of them have quantified the role of temporal modification in structural connectivity induced by land cover changes. In light of these, the main aims of this paper are to quantify the recent (post-1950s) channel changes in the Taro and Ceno rivers and to evaluate the linkage between channel evolutionary trajectories and sediment alterations at catchment and reach scales. More specifically, the following main goals are pursued: i) to reconstruct the evolutionary trajectories of the Taro and Ceno rivers, highlighting similarities and dissimilarities especially in terms of the magnitude of changes; ii) to assess the role of sediment disconnection caused by land use changes along the hillslopes on the post-1950s active channel changes; and iii) to assess the impact of in-channel sediment mining and in-channel work constructions on channel morphology adjustments.

## 2. Study area

The Taro River originates in the Northern Apennines (Italy) and flows for about 126 km in a SW-NE direction, reaching a Strahler stream order of 5. It drains an area of about 2030 $km^2$ before reaching the Po River. The average elevation of the basin is 500 m a.s.l., ranging between 27 m a.s.l. and 1800 m a.s.l. The Ceno River is the Taro's main tributary (*Strahler* stream *order = 4)*, with a total length of about 60 km - it drains a basin area of about 540 $km^2$. Both rivers originate at Mount Penna, the Taro River at about 1500 m a.s.l. and the Ceno River at 1600 m a.s.l. In both catchments, geology consists of dominant sedimentary marine deposits (including sandstones, clays, marls, and limestones) with subordinate ophiolites in the mountainous and hilly portion (approximately 80 % of the total Taro basin) and alluvial deposits in the lower portion of the catchment.

Climate is typical of the temperate areas, characterized by cool and moderately wet winters, hot and dry summers, and wetter springs and autumns. Mean annual precipitation (1991–2020) ranges from a minimum of 790 mm at Coltaro di Sissa weather station (33 m a.s.l.) to a maximum of 1900 mm at Casoni di Santa Maria di Taro (853 m a.s.l.) weather station (Arpae, 2024; Fig. 1). Mean annual discharge is about 30 $m^3$/s for the Taro River and about 15 $m^3$/s for the Ceno River. The most significant flood was recorded in 1982 (peak discharge of 3200 $m^3$/s measured at the Fornovo di Taro gauging station, Fig. 1).

This study focuses on a segment 91-km long of the Taro River, located between Borgo Val di Taro town and the confluence with the Po River, and on a segment 34-km long of the Ceno River, between Bardi town and the confluence with the Taro River (Fig. 1). Based on current channel planform morphology and the presence of tributaries, the two rivers have been divided into homogeneous reaches (Brierley and Fryirs, 2005, Fig. 1). In particular, 23 reaches were analysed along the Taro River (Fig. 1) with channel length ranging from a minimum of 1 km to a maximum of 16 km. From upstream to downstream, the Taro's channel morphology shifts from sinuous with alternate bars or wandering patterns within the confined valley (reaches from 1 to 13, Fig. 1), to braided morphology in the partly-confined (reaches from 14 to 17, Fig. 1) and unconfined valleys (reaches from 18 to 21, Fig. 1). Finally, in the most downstream reaches (22 and 23, Fig. 1), the Taro exhibits a meandering morphology flowing through an unconfined valley (Fig. 1). The Ceno River was divided into 12 reaches (Fig. 1) with length ranging from 1 to 4 km. These reaches, located in confined (reaches from 1 to 9, Fig. 1) or partly-confined valleys (reaches from 10 to 12, Fig. 1), are characterized by braided, wandering, or sinuous with alternate bars patterns.

## 3. Materials and methods

A variety of data from diverse sources and methods were applied in this study to analyse channel changes and the role of related controlling factors (Fig. 2). Multi-temporal orthophotos and topographic surveys were used to quantify channel width and bed level changes (Section 3.1). Land use (Section 3.2) and sediment connectivity (Section 3.3) changes were assessed at the catchment-scale to evaluate the contribution of hillslope processes and sediment sources. The possible role of gravel mining and in-channel works was estimated at the reach-scale by complementing inventories of in-channel human activities (Section 3.4). Precipitation records were analysed to explore climatic influences (Section 3.5). Finally, the available database on seismicity indicates that no significant seismic events occurred during the investigated time interval; therefore, the influence of earthquake-related disturbances on

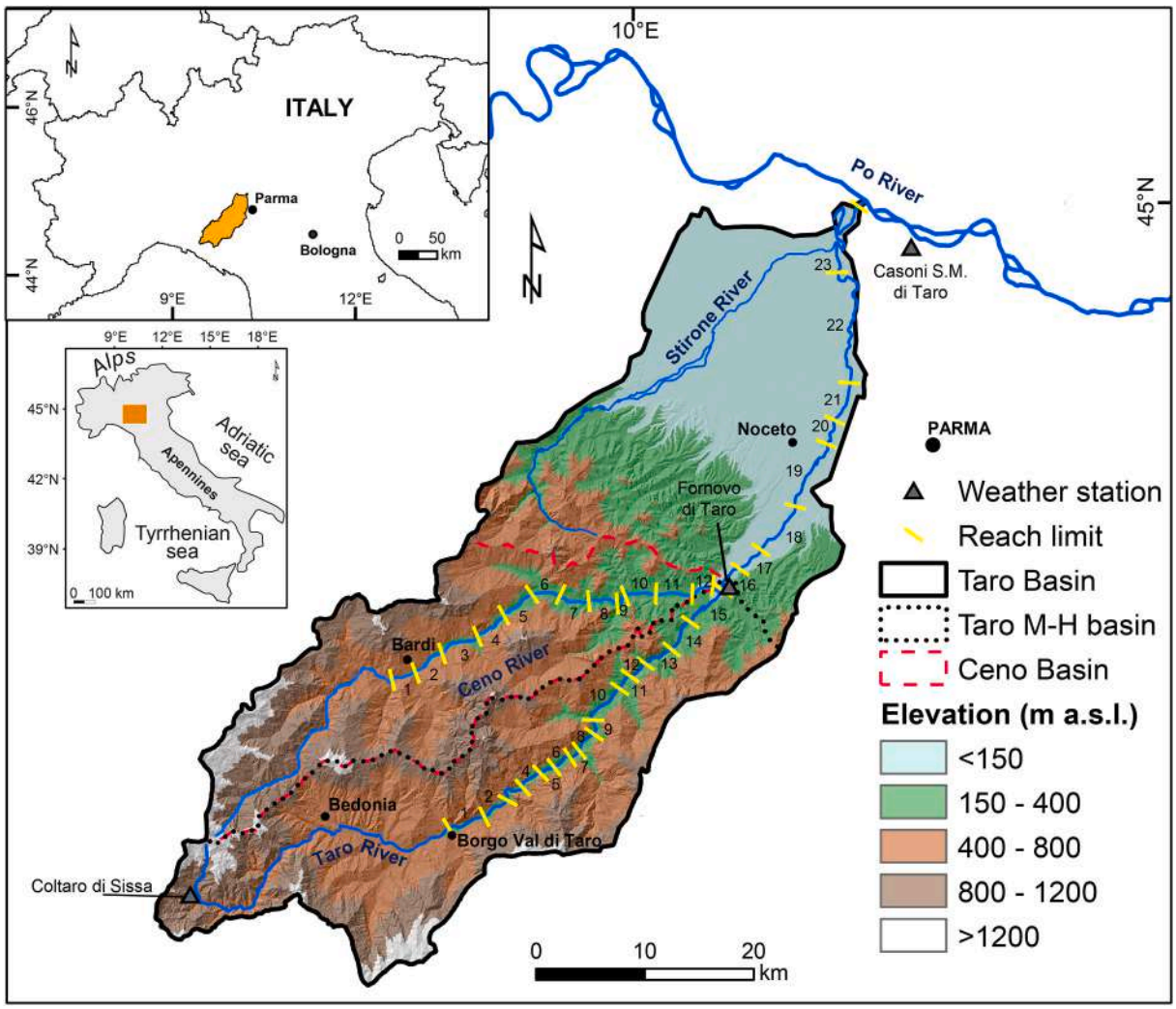



**Fig. 1.** Location of the catchments of the Taro and Ceno rivers, and limits of the studied reaches. Codes: M-H corresponds to the Taro basin mountain-hilly physiographic unit.

channel and sediment dynamics can be excluded for this analysis.

### 3.1. Analysis of channel width and bed level changes

Multi-temporal analyses on active channel width changes were performed in GIS environment from 1954 to 2020, using five sets of orthophotos (i.e., 1954, 1976, 1988, 1996 and 2020; Table 1). Channels were manually digitized as polygons, excluding the islands from the active channel areas. The average active channel width ($W$) was calculated for each year at reach-scale using the following equation:

$$Wi = Ai/Li \quad (1)$$

where for a reach ($i$), $A$ is the area of the polygon that outlines the active channel and $L$ is the length of the middle axis.

In order to compare the channel evolution of the two rivers, changes in active channel width were calculated with respect to the active channel width in 1954 (the oldest orthophoto available) using the following equation:

$$\Delta W_{1954}\ (\%) = -(1 - W/W_{1954})*100 \quad (2)$$

where $W$ is the average active channel width measured in different years (i.e., 1976, 1988, 1996, and 2020), and $W_{1954}$ is the average active channel width in 1954. In order to gain a deeper insight into the evolutionary processes of the two rivers, analysis of changes in bed elevation was conducted using topographical cross- sections carried out in 2005 (39 along the Taro and 5 along the Ceno) and accessible on the website of the *Agenzia Interregionale per il fiume Po* (AIPO, 2024), since other long-term topographic data were not available. Bed level changes between 1954 and 2005 were estimated considering the lateral shifts of the active channels in the post-1950s and comparing differences in elevation between some geomorphic surfaces (e.g., floodplains, bars, active channel) clearly identified from orthophotos for both years (1954 and 2005).

### 3.2. Land use changes at the catchment scale

Land use changes were evaluated at the catchment scale in the mountain-hill basin of the Taro River (i.e., from reach 1 to reach 15, up to the confluence with the Ceno River) and in the Ceno basin (Fig. 1), using four land cover maps (1954, 1976, 1994, 2020) available on the regional geoportal (Table 1; Geoportale Regione Emilia-Romagna, 2024b). Starting from the Corine land cover classification, land use was reclassified into six main categories: (i) artificial surfaces, (ii) agricultural areas, including crops mainly characterized by cereals, areas with cultivated trees and crops with cultivated trees, (iii) forests, (iv) shrubs and/or herbaceous vegetation associations, (v) open spaces with little or no vegetation, and (vi) water bodies.

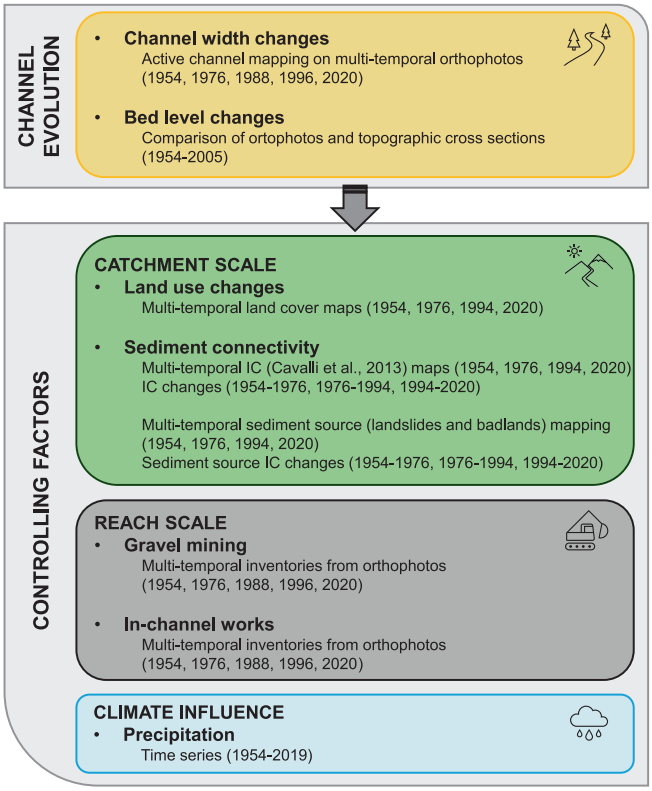



**Fig. 2.** Flowchart of methods and materials used in this study to analyse channel changes and related controlling factors.

**Table 1**
Material used for the analysis.

| Type | Year | Pixel size (m) | Bands | Source |
|---|---|---|---|---|
| Orthophoto | 1954 | 1 | B&W | WMS *E*-R** |
| Orthophoto | 1976 | 0.3 | RGB | WMS E-R** |
| Orthophoto | 1988 | 1 | B&W | WMS GN* |
| Orthophoto | 1996 | 1 | B&W | WMS GN* |
| Orthophoto | 2020 | 0.2 | RGB | WMS E-R** |
| Land cover shapefile | 1954 | – | – | E-R*** |
| Land cover shapefile | 1976 | – | – | E-R*** |
| Land cover shapefile | 1994 | – | – | E-R*** |
| Land cover shapefile | 2020 | – | – | E-R*** |
| DTM | 2009 | 5 | – | E-R**** |

* GN (Geoportale Nazionale, 2024).
** E-R (Geoportale Regione Emilia-Romagna, 2024a).
*** E-R (Geoportale Regione Emilia-Romagna, 2024b).
**** E-R (Geoportale Regione Emilia-Romagna, 2024c).

### 3.3. Connectivity index and sediment sources

Multi-temporal maps based on the Index of sediment Connectivity (IC), originally developed by Borselli et al. (2008) and modified by Cavalli et al. (2013), were carried out to evaluate the potential cascade of sediments between hillslopes and the main channels. The IC is estimated as:

$$IC = log_{10}\left(\frac{D_{up}}{D_{dn}}\right) \quad (3)$$

where $D_{up}$ and $D_{dn}$ are respectively the upslope and downslope components of connectivity. The upslope component ($D_{up}$) represents the potential for the sediment produced upslope to be transported in a downward direction. It is evaluated as follows:

$$D_{up} = WS\sqrt{A} \quad (4)$$

where $W$ is the average weighting factor, $S$ is the average slope gradient (m/m), and $A$ is the upslope contributing area ($m^2$). The downslope component ($D_{dn}$) considers the flow path length (modified by a weighting factor) that a particle has to travel to reach the closest target or sink. This is estimated as follows:

$$D_{dn} = \sum_i \frac{d_i}{W_i S_i} \quad (5)$$

where $d_i$ is the length of the flow path along the $i^{th}$ cell (m), $W_i$ is the weighting factor and $S_i$ is the slope gradient of the $i^{th}$ cell.

In this work, the IC maps were computed using the software SedInConnect 2.3 (Crema and Cavalli, 2018). The maps were obtained by setting a 5-m resolution DTM, taken in 2009 and available from the Emilia Romagna Region Geoportal (Geoportale Emilia-Romagna, 2024c; Table 1). In accordance with the original methodology by Cavalli et al. (2013), two different targets were chosen: the first concerning the Ceno active channel up to the confluence with the Taro, and the second considering the Taro River in the mountain-hilly segment, upstream to the confluence with the Ceno River (reaches from 1 to 15, Fig. 1). These allowed us to analyse the probability that sediments eroded from the hillslopes could reach the drainage network, and particularly the two main channels. Although multi-temporal DTMs were not available for the study area, the integration of multi-temporal land use maps permitted us to capture the main temporal dynamics influencing structural sediment connectivity. In light of this, land use changes were integrated in the IC computation, using land use maps in 1954, 1976, 1994 and 2020 (see Section 3.2). The weighting factor ($W$), based on the Manning's Roughness coefficient as in Persichillo et al. (2018), was set to model the impedance to water and sediment flux related to each land use class (Table 2). Maps of IC changes were carried out and reclassified into four classes (High decrease, Low decrease, Low increase, and High increase) to estimate the changes of structural connectivity from 1954 to 2020. Following Llena et al. (2024), the limit between classes was defined using the zero value and those corresponding to ± the standard deviation. The same criteria were applied to reclassify the maps of IC change in the analysed periods.

In order to analyse the changes in sediment supplied to the two rivers derived from mass wasting processes along the hillslopes, sediment sources (i.e., landslides and badlands) were mapped using orthophotos of 1954, 1976, 1996 and 2020 (Table 1). Starting from the multi-temporal mapping of sediment sources, obtained geomorphological maps were overlapped to the multi-temporal connectivity index maps. This allowed us to assess changes in sediment source areas and their connectivity to the two rivers over the investigated period.

### 3.4. Gravel mining and in-channel work construction

To evaluate the impact of human activities on the channel changes in the two rivers, the occurrence of gravel extractions and in-channel works - in the two main channels - were mapped using the available orthophotos (Table 1). Two multi-temporal inventories were implemented for each river, the first documenting areas affected by gravel

**Table 2**
Weighting factor (W) assigned to each land use class (modified from Persichillo et al., 2018).

| Land use class | Weighting factor (W) |
|---|---|
| Artificial surfaces | 0.98 |
| Agricultural areas | 0.80 |
| Forests | 0.60 |
| Shrubs and/or herbaceous vegetation associations | 0.70 |
| Open spaces with little or no vegetation | 0.95 |

mining and the second recording the presence of in-channel works. Both inventories were carried out at reach scale in GIS environment. Gravel mining activity areas were mapped within the floodplain and in the active channel. In-channel works were classified into transversal or longitudinal.

### 3.5. Hydrological and precipitation data

Long-term discharge data are not available for the two analysed rivers. However, peak discharge values are documented for some flood events that caused the most intense impact on anthropic buildings, as reported in Table 3. Due to the lack of continuous hydrometric records, this study focused on precipitation data, available on the "Annali idrologici" (Arpae, 2024) for the period 1954–2019, with a gap between 1996 and 2000. Daily and maximum monthly precipitation records were analysed. To investigate possible temporal trends, the dataset was divided into four time periods, according to the availability of orthophotos for the analysis of the channel dynamic: (i) from 1954 to 1975 (T1), (ii) from 1976 to 1987 (T2), (iii) from 1988 to 1993 (T3), and (iv) from 2001 to 2019 (T4). Statistical differences between the four time periods were tested applying the pairwise non-parametric Mann-Whitney test. Statistical significance was set to $p$-value $<0.05$. Analyses were conducted within the statistical software R version 4.0.0 (R Core Team, 2020).

## 4. Results

### 4.1. Channel width and bed level changes

Analyses of the active channel width changes highlighted similarities but especially important differences in the evolution of the Taro and Ceno rivers. Both rivers exhibited the maximum active channel width in 1954 (Figs. 3A, B, 4A and B), with median values of about 200 m in the Taro and 225 m in the Ceno. Maximum channel width attained about 1360 m in the Taro (reach 17, Fig. 3A) and about 500 m in the Ceno River (reach 10, Fig. 3B). After the 1950s in the Taro, the average active channel width decreased by about −43 % between 1954 and 1976, and then it presented values oscillating between −27 % (in 1988) and −50 % (in 1996) with respect to 1954 (Fig. 4A). In 1988, most reaches showed evidence of channel width widening (Fig. 3A) and channel morphology recovery, even though widths in 1954 were not retrieved. The Ceno River instead exhibited a progressive narrowing from 1954 forward, up to −38 % in 1996, with respect to 1954 (Figs. 3B and 4B). In both rivers, minimum active channel widths were estimated in 1996 (Figs. 3A, B, 4A and B) and then, the channel narrowing was followed by a slight widening between 1996 and 2020 (+16 % in the Taro River and +12 % in the Ceno River). Analysis clearly showed that active channel narrowing was more intense in the Taro River all along the entire investigated time period (Figs. 3 and 4).

In the Taro, active channel changes were analysed also with respect to the lateral confinement, according to the three valley settings differentiated by Brierley and Fryirs (2005): confined reaches (reaches from 1 to 13, Figs. 3A and 4C); partly-confined (reaches from 14 to 17, Figs. 3A and 4D); and laterally unconfined (reaches from 18 to 23, Figs. 3A, 4E and F). Narrowing was less intense in the confined reaches (Fig. 4C) with respect to the partly-confined (Fig. 4D) and especially the unconfined reaches (Fig. 4E). In particular narrowing increased from upstream (confined valley, Fig. 4C) to downstream (unconfined valley, Fig. 4E), except for reaches 22 and 23, that exhibited limited changes (Fig. 4F) due to the presence of bank defence works, since the 1950s. In contrast, the Ceno River did not display any clear distinction of active channel changes based on the valley confinement. Finally, it is relevant to notice that if on one hand the evolution of the two rivers is quite different especially in terms of magnitude of changes, on the other hand percentage of changes estimated in the Ceno (Fig. 4B) are very similar to those found in the confined reaches of the Taro, located in the upper-medium part of the basin (Fig. 4C).

In both rivers, morphological analysis indicates prevalence of single-thread patterns in the confined reaches and multi-thread or transitional patterns in the partly-confined and unconfined reaches (Fig. 5A, B and C). Multi-thread and transitional patterns prevailed throughout the whole examined period (Fig. 5D and E). In the Taro, sinuous and straight reaches appeared in 1976 and peaked in 1996 (Fig. 5A and D), while meanders remained stable at reaches 22 and 23, since 1954 (Fig. 5E). The Ceno River displayed exclusively multi-channel and transitional morphologies (Fig. 5C and E). In particular, braided reaches have been consistently the predominant morphology, accounting for more than 50 %, except for 1996, when their presence temporarily decreased to 42 % (Fig. 5C and E). Finally, in both rivers, an increase in braided patterns in the partly-confined and unconfined reaches, and in sinuous with alternate bars patterns in the confined reaches was observed in 2020 (Fig. 5D and E).

Analysis of topographic sections (Fig. 6A and B) reveals that both rivers have incised since 1954. Bed level variations in the Taro River resulted in a median incision of approximately −3.3 m (Fig. 6C). In the Ceno River, due to limited availability of cross-sections, bed level changes were measured only at the reaches 4, 7, 8, and 10. Here, the median incision was approximately −2.5 m (Fig. 6C), with maximum values of −3.6 m at the most upstream reach (reach 4) and of about −2.4 m in the other reaches located downstream. Considering both rivers, analysis highlighted no significant relation between bed level changes and changes in channel width expressed by means of the ratio between the minimum ($W_{min}$, in 1996) and the maximum ($W_{max}$, in 1954) active channel width (Fig. 6D). In the Taro, as illustrated in Fig. 6E, incision was more intense in the reaches located upstream (reaches from 1 to 11), where the channel is confined. Here, incision ranged between −3 and −7 m (at reach 8, Fig. 6E) with median values of −5 m. In the partly-confined and unconfined reaches (reaches from 16 to 21), incision was less intense (median value −3 m) and oscillated between −0.6 m (reach 18, Fig. 6E) and −7 m (reach 21, Fig. 6E).

**Table 3**
Main flood events in the Taro basin.

| Data | Discharge ($m^3/s$) | Station/Location | Source |
|---|---|---|---|
| 15/10/1953 | 438 | Piane di Carniglia (Taro) | AdBPo, 1999 |
| 11/12/1959 | 167 | Ponte Strambo (Taro) | AdBPo, 1999 |
| 05/09/1963 | 340 | Santa Maria (Taro) | AdBPo, 1999 |
| 09/11/1982 | 3200 | Fornovo (Taro) | AdBPo, 1999 |
| 09/11/1982 | 2000 | San Quirico (Taro) | AdBPo, 1999 |
| 11/11/2014 | 1100 | San Secondo (Taro) | AdBPo, 2024; Arpae, 2024 |
| 12/12/2017 | 1280 | San Secondo (Taro) | AdBPo, 2024; Arpae, 2024 |
| 03/11/2019 | 522 | San Secondo (Taro) | AdBPo, 2024; Arpae, 2024 |
| 23/01/2021 | 1210 | San Secondo (Taro) | AdBPo, 2024; Arpae, 2024 |

### 4.2. Catchment scale factors controlling channel morphology

#### 4.2.1. Land use changes

Multi-temporal maps of land use over the investigated time period allowed us to analyse land use changes at catchment scale. The 1954 maps revealed the prevalence of forests in both catchments, respectively 53 % of the basin area in the Taro and 45 % in the Ceno (Fig. 7), followed by agricultural areas (about 30 % in both basins, Fig. 7). In both catchments, an increase in forests and a decrease in agricultural areas was observed over time and especially after the 1970s (Fig. 7). In

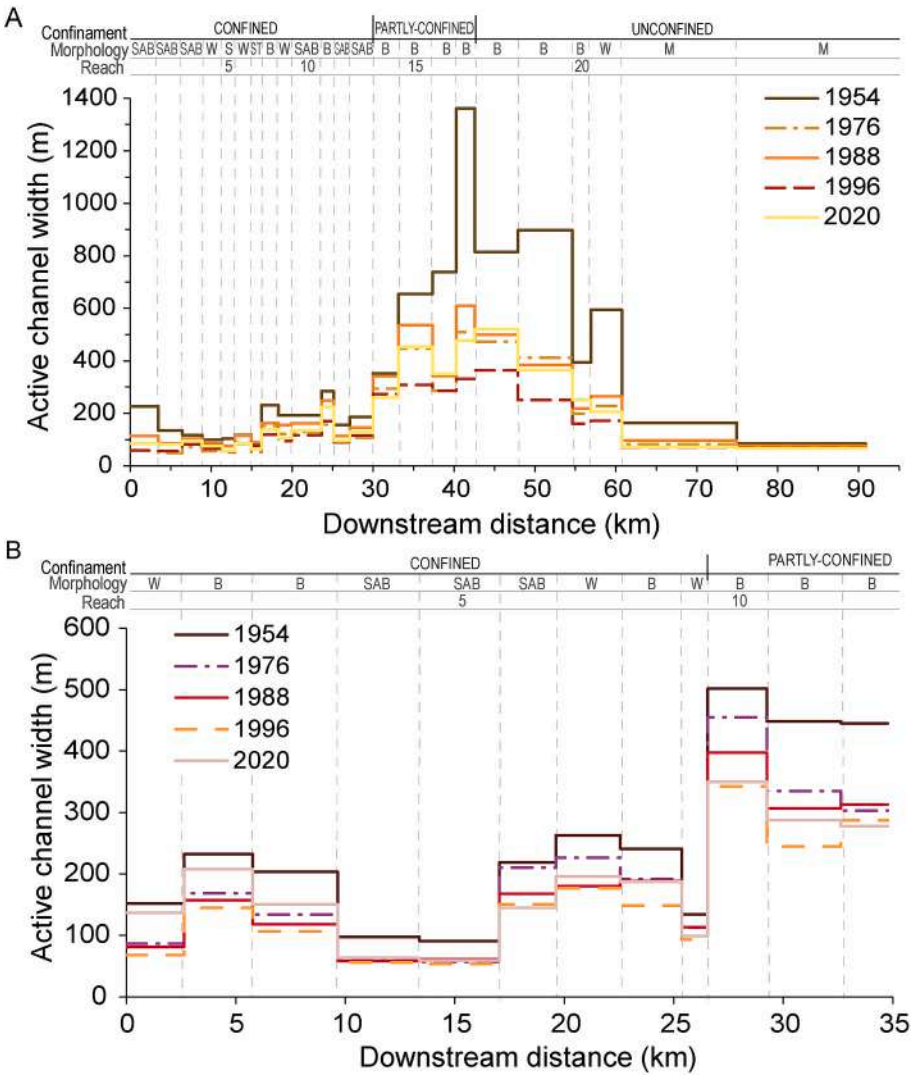



**Fig. 3.** Multi-temporal variation from upstream to downstream of the active channel width at the reach-scale in the (A) Taro and (B) Ceno rivers. Channel morphology codes, referring to 2020: ST = straight; S = sinuous; SAB = sinuous with alternate bars; M = meandering; W = wandering; B = braided.

particular, in the Taro basin, forest growth increased after the 1970s (+1 % in 1976 and +16 % in 1994, Fig. 7A), mostly replacing agricultural areas (Fig. 7A). In the Ceno basin, forests increased after the 1950s (+9 % in 1976 and +13 % in 1994, Fig. 7B), with corresponding decrease in shrubs and/or herbaceous associations (−8 %) in 1976 and in agricultural areas (−9 %) in 1994 (Fig. 7B). After the 1970s both basins showed the same trends, and land cover remained relatively stable (Fig. 7). Currently (2020), forests predominate in both catchments, accounting for approximately 69 % of the catchments' area. In summary, the land cover characteristics and changes since the 1950s were quite similar in the Taro and Ceno basins. The only difference consisted in the fact that forests increased immediately after 1954 in the Ceno and some decades later (after the1970s) in the mountain-hilly Taro basin.

#### 4.2.2. *Structural connectivity and sediment sources changes*

Analysis of structural connectivity over time – performed through the IC - shows a gradual increase of areas with high and low decrease in IC (blueish colours in Fig. 8) and the relative decrease of areas with low and high increase in IC (reddish colours in Fig. 8), resulting in the overall reduction of the sediment connectivity to the Taro and Ceno channels (Fig. 8). Values of IC appeared quite similar among the two basins during all analysed years (Fig. 8). Sediment connectivity lowering in the Taro catchment had already started in 1976, in comparison with 1954 (Fig. 8A and D), but it particularly decreased after 1994 (Fig. 8C and D). A similar trend is detected in the Ceno catchment, where a significant increase in disconnected areas was observed in the period 1994–2020 (Fig. 8C and D).

The strength of coupling between neighbouring storages on hillslopes and the two main rivers decreased over time from upstream to downstream. From 1954 to 1976 connected and disconnected areas were quite uniformly distributed in the two catchments (Fig. 8A), whereas in the period 1976–1994 upland landforms resulted disconnected and the middle-low part of the basins remained connected (Fig. 8B). Finally in the period 1994–2020, most basin areas were mainly disconnected (Fig. 8C).

Analysis of sediment sources evolution over time (landslides and badlands) and relative connectivity to the Taro and Ceno channels also highlighted a decrease in sediment supply. The 1954 sediment source inventory featured an area of almost 80 $km^2$ in the Taro Basin and of 60 $km^2$ in the Ceno Basin, corresponding to approximately 11 % of both catchments' area. The sediment production areas decreased, especially since 1976, and remained stable after 1996 (Table 4 and Fig. 9). Over time, and especially after 1994 in both catchments, the sediment sources located in areas characterized by low connectivity increased (areas showing high and low decrease in IC; Fig. 9E, F, G and H), while those

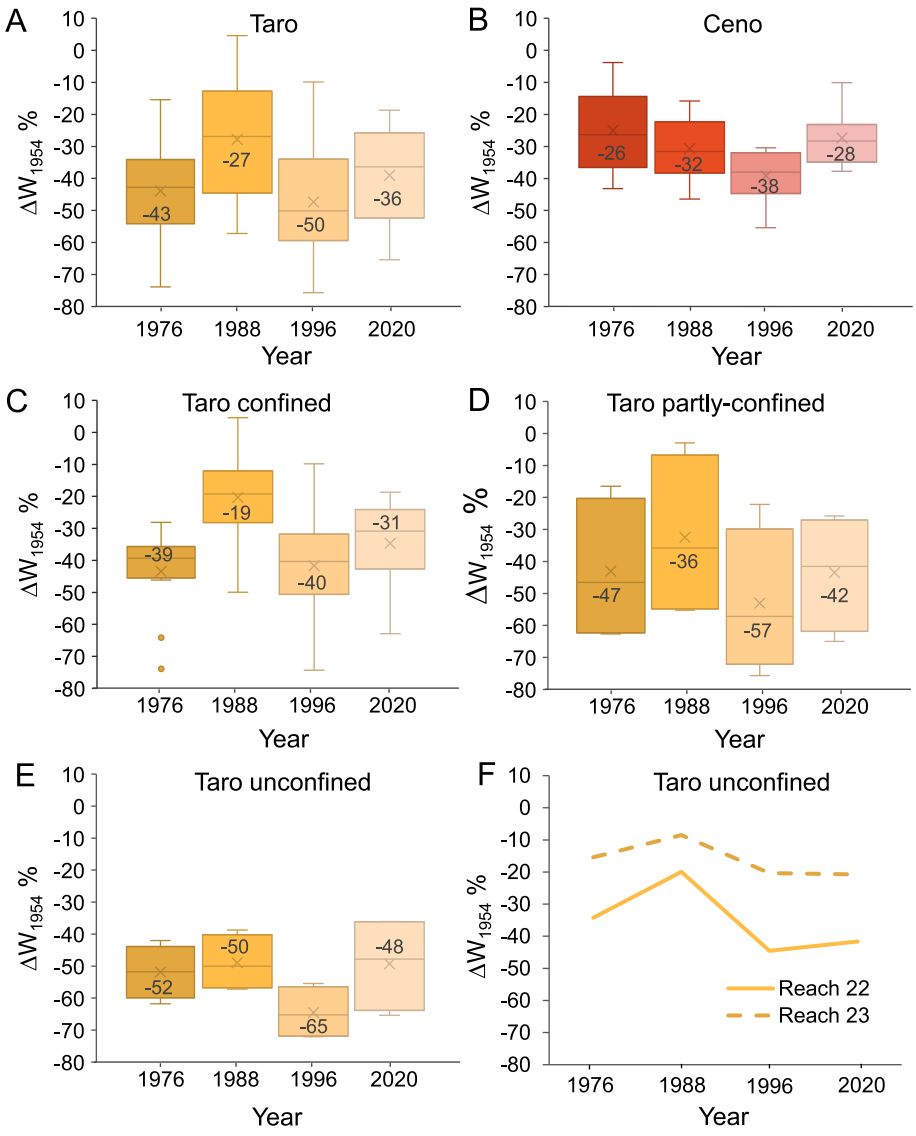



**Fig. 4.** Multi-temporal variation of the active channel width with respect to 1954 in: the (A) Taro and (B) Ceno rivers; the (C) confined (reaches 1–13), (D) partly-confined (reaches 14–17), and (E, F) unconfined (reaches 18–21 and reaches 22 and 23, respectively) reaches of the Taro River.

located in areas with high connectivity decreased (areas showing high and low increase in IC; Fig. 9E, F, G and H).

### 4.3. *Reach scale controlling factors: gravel mining and in-channel works*

Gravel mining started in both catchments in the 1970s and was detected mainly in the floodplains of both rivers. In-channel mining activities were observed in the 1976 orthophoto only within the Taro active channel (Figs. 5B in 1976 and 10A), for a total area of approx. 1 $km^2$, while no evidence was found in the Ceno active channel (Fig. 10A). Mining areas identified on the Taro floodplains decreased from a maximum of approx. 3 $km^2$ in 1976 to a minimum of 0.8 $km^2$ in 2020 (Fig. 10A). In the Ceno floodplains, the extent of mining areas was comparatively smaller, as it increased from 0.06 $km^2$ in 1976 to approx. 0.1 $km^2$ in 1988 and 1996, and then decreased to 0.07 $km^2$ in 2020 (Fig. 10A). In-channel gravel extraction was officially banned by law, in 1982. Taro's reaches impacted by gravel mining exhibited a greater degree of channel narrowing between 1954 ($W_{max}$) and 1996 ($W_{min}$), compared to those not affected (Fig. 10B). In-channel gravel mining activity was widespread along the entire Taro River, but particularly in the partly-confined reaches (reaches 18–21, Fig. 10C). Notably, reaches 19 (~ 0.7 $km^2$ of mining area, see also Fig. 5B) and 21 (~ 0.3 $km^2$ of mining area) - characterized by multi-channel and transitional morphology -presented the most extensive mining areas (Fig. 10C).

In the Taro River, some localized bank protections have been present since the 1950s. Check-dams, built since the 1970s, represent the most prevalent works in the upstream and confined reaches (reaches 1, 5, 7, and 8; Fig. 10C). Number of check dams gradually decreases downstream; conversely the presence of bank protection structures increases in the reaches from 21 to 23, where the channel presents mainly a meandering pattern (Fig. 10C). Embankment account for about 38 % of banks at reach 22 and 71 % of the banks at reach 23. In contrast, there is no evidence of in-channel work constructions in the Ceno River.

Overall, channel bed incision was slightly more intense in the reaches affected by anthropic activities (gravel mining and/or construction of channel work, median value −3.3 m, box and whiskers plots in Fig. 10C) compared with reaches without evidence of direct in-channel human impact (median value −2.8 m, box and whiskers plots in Fig. 10C).

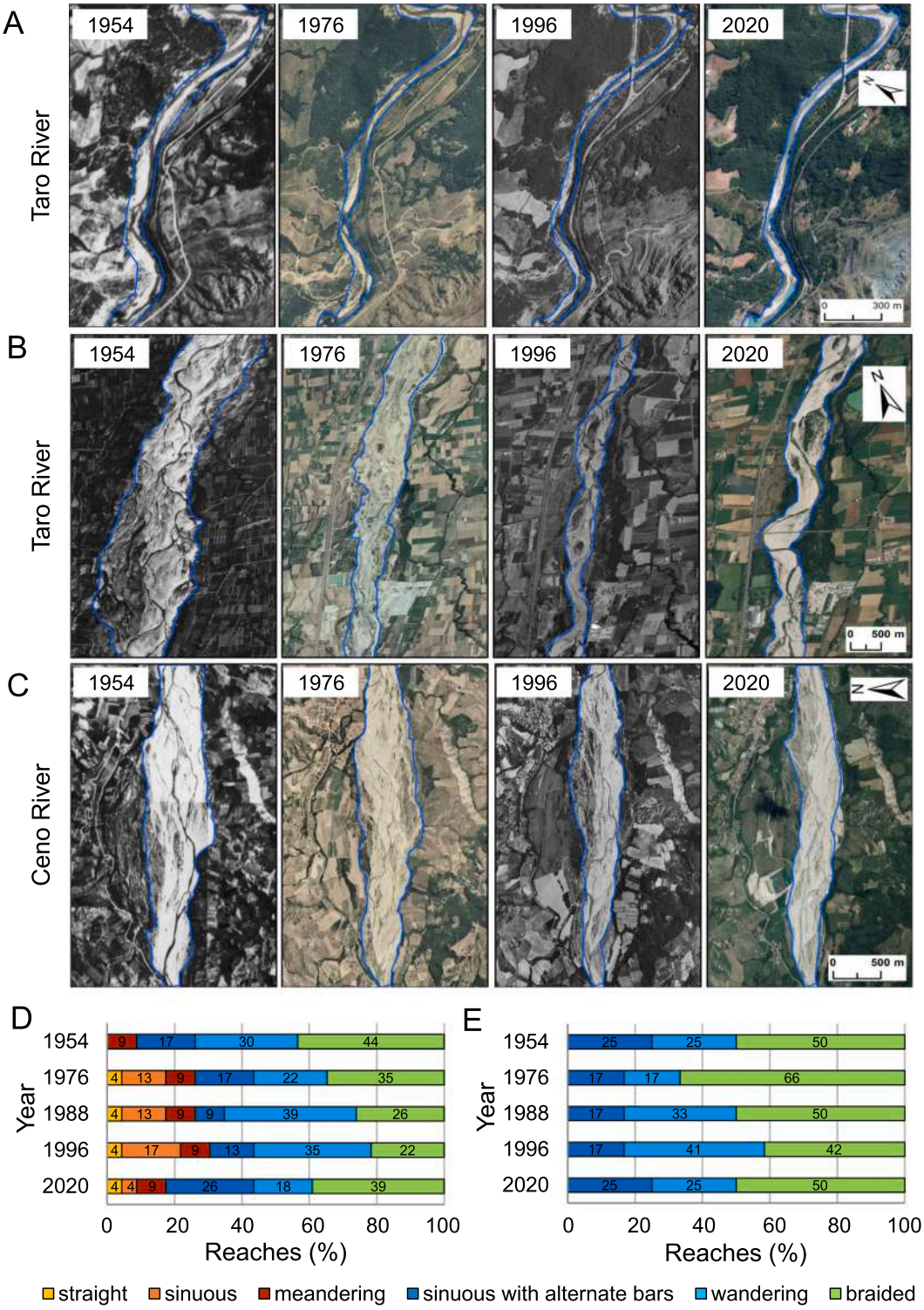



**Fig. 5.** Multi-temporal orthophotos showing morphological variation in channel width and pattern: (A) at a single-thread reach (reaches 5), (B) at a multi-thread reach (reach 19) of the Taro River and (C) at reach 2 of the Ceno River. Pattern distribution (% of reaches) from 1954 to 2020 in (D) the Taro and in (E) the Ceno rivers.

### *4.4. Precipitation analysis*

The temporal variations of daily and maximum monthly precipitation did not differ significantly from 1954 to 2019 ($p$-value >0.05). The median values of daily precipitation remain relatively stable (about 4 mm/day) during the intervals 1954–1975 (T1), 1976–1987 (T2) and 1988–1993 (T3), while a slight, but not statistically significant decrease (3 mm/day) was observed in the interval 2000–2019 (T4, Fig. 11A). Only a slight decrease in median values of maximum monthly precipitation was observed from T1 and T2 (27 mm/month) to T3 (23 mm/month), and a slight increase in T4 (29 mm/month; Fig. 11B). In summary, precipitation showed stationary trends, except for a small increase in the last two decades (2001–2019).

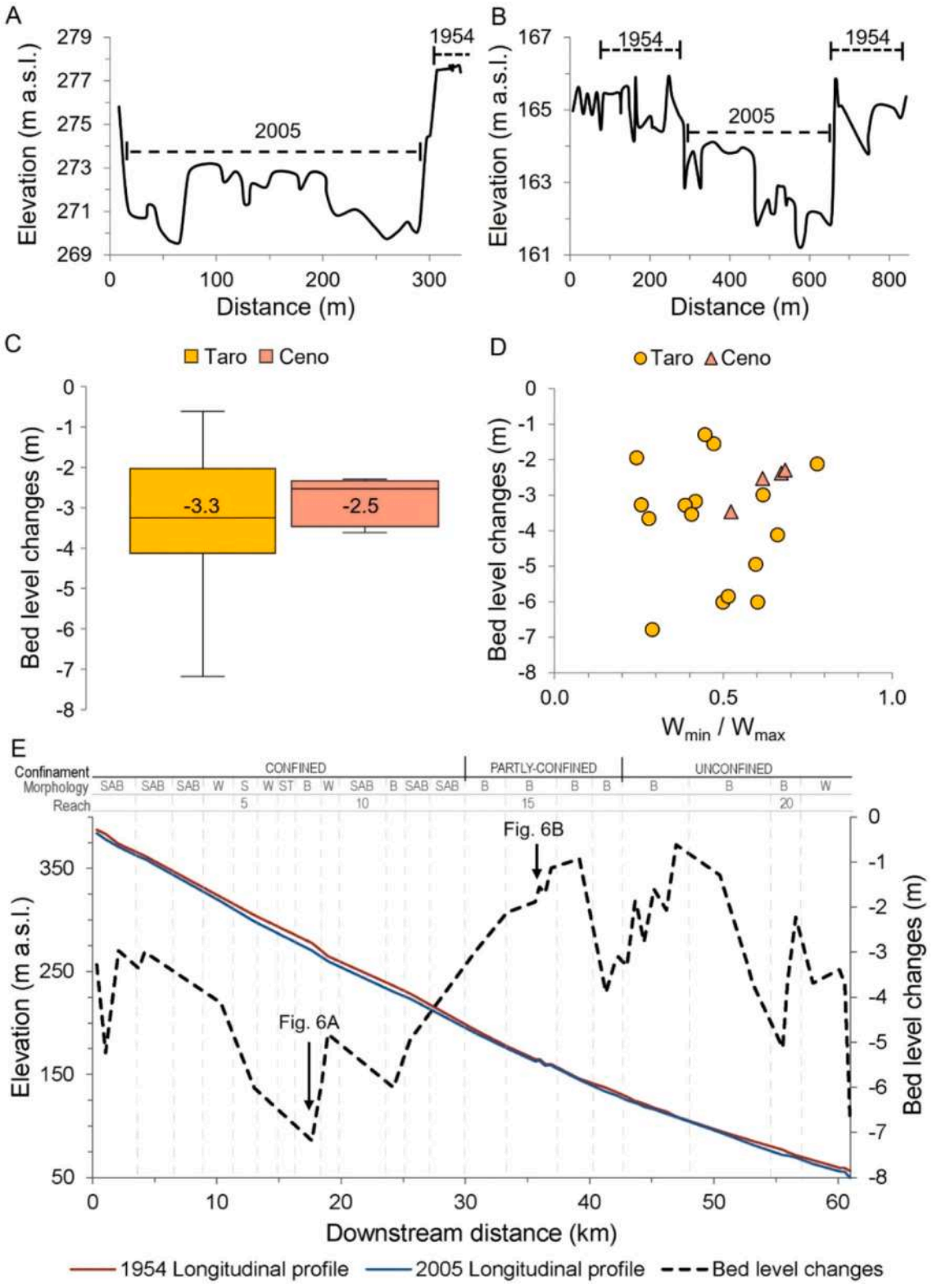



**Fig. 6.** Example of topographic cross-sections showing channel incision in the Taro River, at reaches 8 (A) and 15 (B) over the period 1954–2005. (C) Box and whiskers plots of bed level changes between 1954 and 2005 in the Taro and Ceno rivers. (D) Scatterplot of the ratio between bed level changes and active channel width changes ($W_{min}/W_{max}$). (E) Longitudinal profiles (from reach 1 to reach 21) of the Taro River in 1954 and 2005, and bed level changes between 1954 and 2005. Channel morphology codes, referring to 2020: ST = straight; S = sinuous; SAB = sinuous with alternate bars; W = wandering; B = braided.

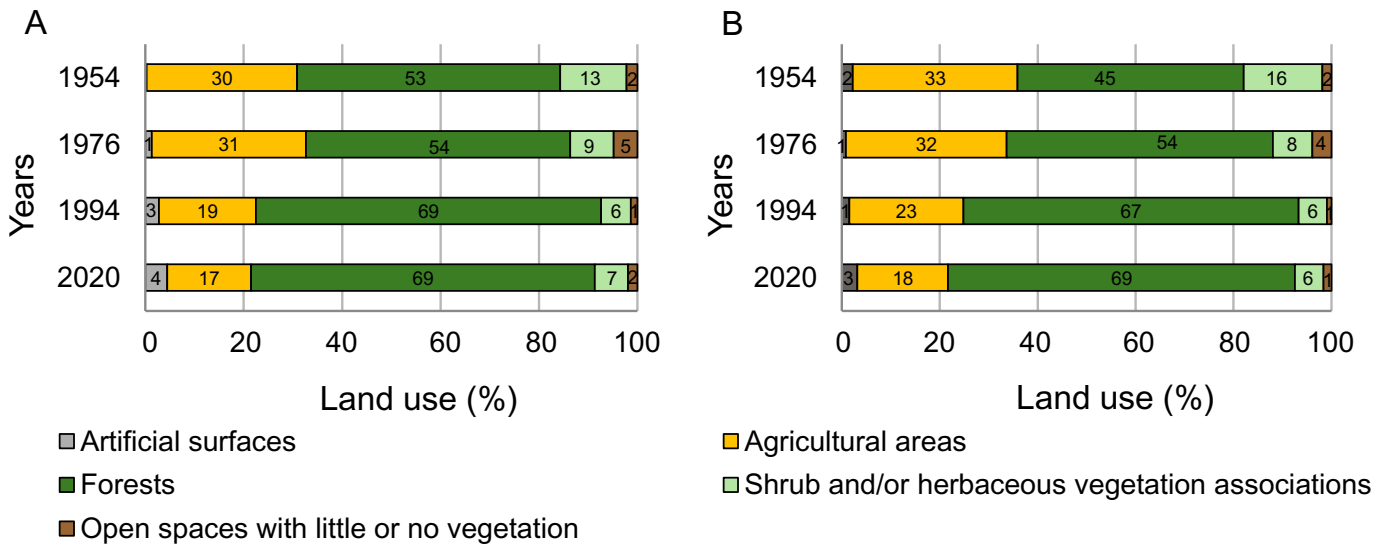



**Fig. 7.** Land use changes between 1954 and 2020 in the (A) mountain-hilly Taro and (B) Ceno catchments.

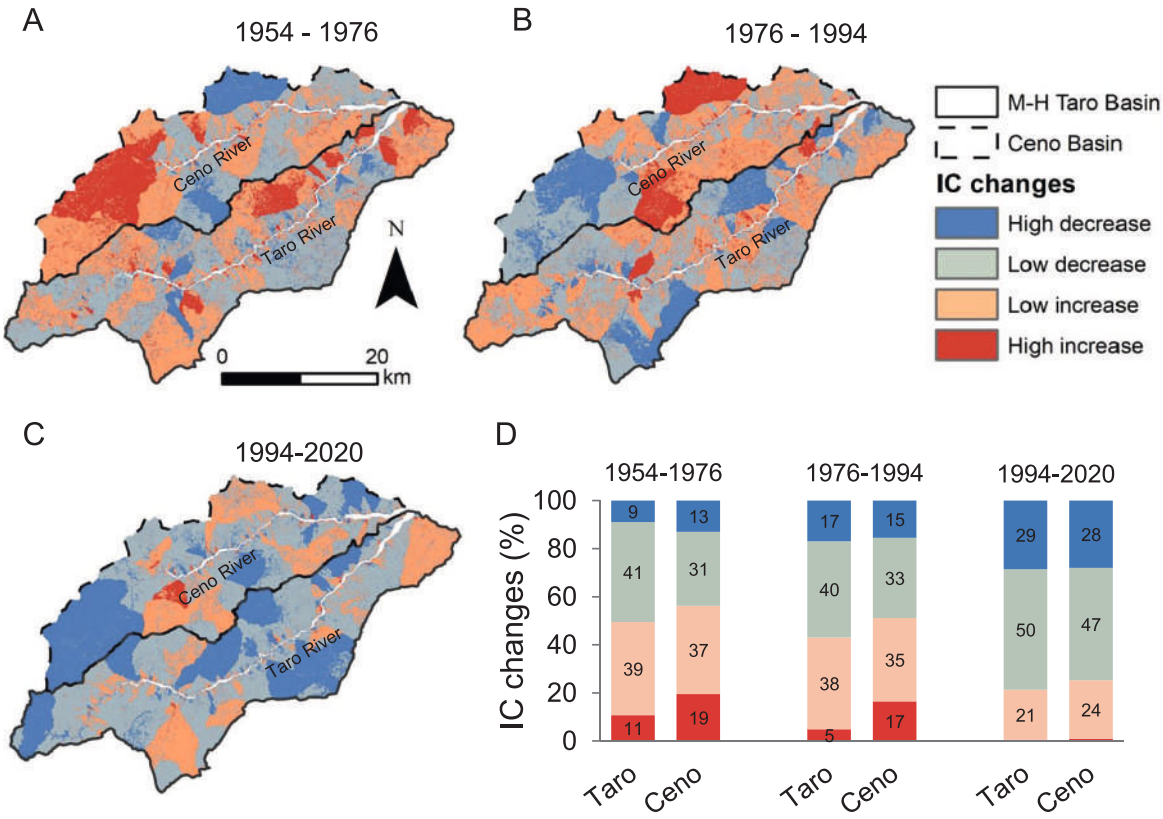



**Fig. 8.** Maps of IC changes in the period (A) 1954–1976, (B) 1976–1994, and (C) 1994–2020. (D) Frequency of IC changes in the 1954–1976-, 1976–1994, and 1994–2020 time intervals in the mountain-hilly Taro and Ceno catchments.

## 5. Discussion

### *5.1. Similarities and dissimilarities in the recent evolutionary trajectories of the Taro and Ceno channels*

Evolutionary trajectories of the Taro and Ceno active channels exhibit many similarities and dissimilarities. Both rivers underwent narrowing, incision and simplification of the channel pattern with respect to 1954 and reached minimum active channel width and morphological complexity in 1996, with the decline of braided and wandering patterns (Figs. 3A, B, 5D, and E). Noteworthy, the main differences between the two rivers consisted of the magnitude of changes, significantly more pronounced in the Taro River. Between 1954 and 1996, the Taro experienced an average channel narrowing of −50 %, with a peak of −76 % in 1996 (Fig. 4A), and a median incision of −3.3 m, with maximum bed level lowering of −7 m (Fig. 6C). The Ceno River showed an average narrowing of −38 %, a maximum active channel decrease of −55 % in 1996 (Fig. 4B) and median and maximum incisions of −2.5 m and −3.5 m, respectively (Fig. 6C). In more detail, morphological changes found in the confined reaches of the Taro River

**Table 4**
Area ratio ($A_i/A_{1954}$) of sediment sources areas of the mountain-hilly Taro and Ceno catchments over time.

| | Area ratio ($A_i/A_{1954}$) | |
|---|---|---|
| Year | Taro | Ceno |
| 1976 | 0.72 | 0.63 |
| 1996 | 0.38 | 0.35 |
| 2020 | 0.31 | 0.34 |

Codes: $A_i$ = sediment sources area in a specific year (1976, 1996, 2020); $A_{1954}$ = sediment sources area in 1954.

were similar to those observed in the Ceno River (Figs. 4B, C and 12), denoting some similarities in the controlling factors that induced observed channel adjustments (see Sections 5.2 and 5.3). In contrast, the partly-confined and unconfined reaches of the Taro River showed significantly greater morphological changes, with average channel narrowing of −57 % in partly-confined and −65 % in unconfined reaches, recorded in 1996 (Fig. 4D and E). These results indicate a progressive downstream intensification of channel degradation along the Taro River, as found in other studies (Liébault et al., 2005; Scorpio and Piégay, 2021).

Notably, the Taro River had already experienced greater narrowing than the Ceno River between 1954 and 1976 (median values: −39 % in the confined reaches, −47 % in the partly-confined reaches, and −52 %

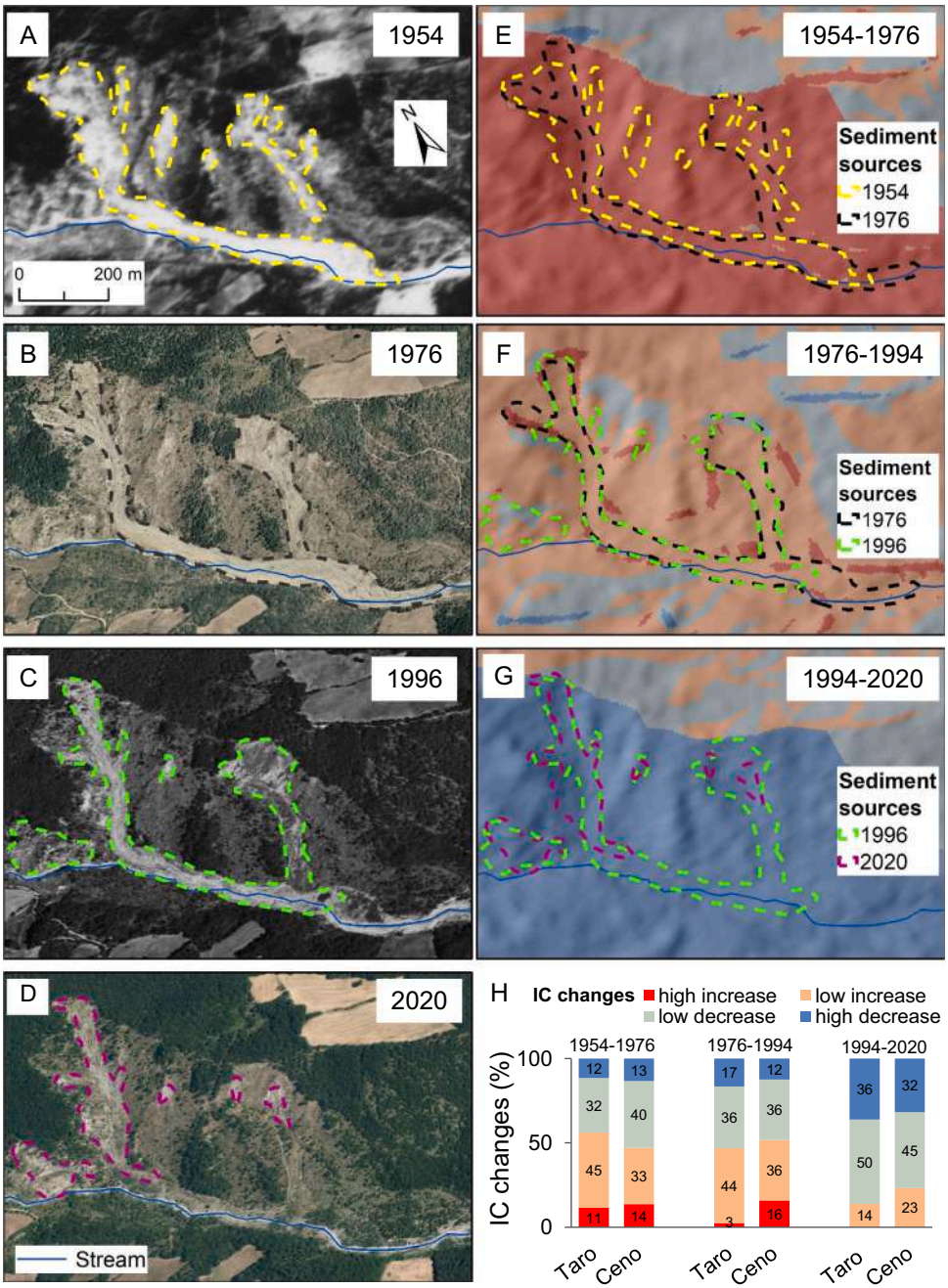



**Fig. 9.** Example of sediment sources evolution in (A) 1954, (B) 1976, (C) 1996, and (D) 2020, and their IC changes between (E) 1954 and 1976, (F) 1976 and 1994, (G) 1994 and 2020. (H) Frequency of sediment sources IC changes in the 1954–1976, 1976–1994, and 1994–2020 time intervals in the mountain-hilly Taro and Ceno catchments.

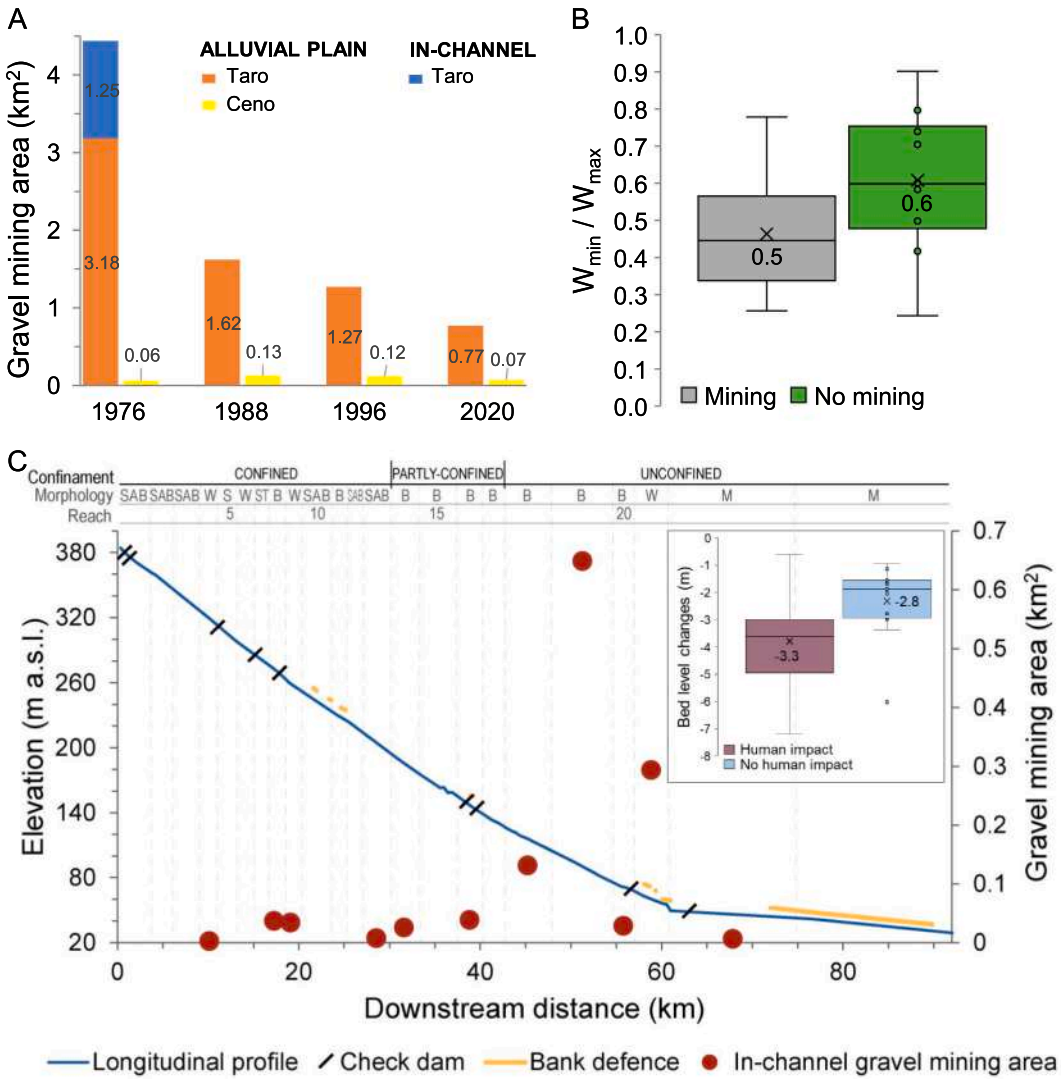



**Fig. 10.** (A) Area of gravel mining extraction in-channel and in the floodplain of the Taro and Ceno rivers. (B) Box and whiskers plots of the active channel width ratio between $W_{max}$ (1954) and $W_{min}$ (1996) in reaches of the Taro River affected and not affected by gravel mining activities. (C) Longitudinal profile and location of in-channel works (check dams and bank defences) and in-channel gravel mining area in the Taro River. Box and whiskers plots represent bed level changes in reaches affected and not affected by gravel mining and/or construction of channel works. Channel morphology codes, referring to 2020: ST = straight; S = sinuous; M = meandering; SAB = sinuous with alternate bars; W = wandering; B = braided.

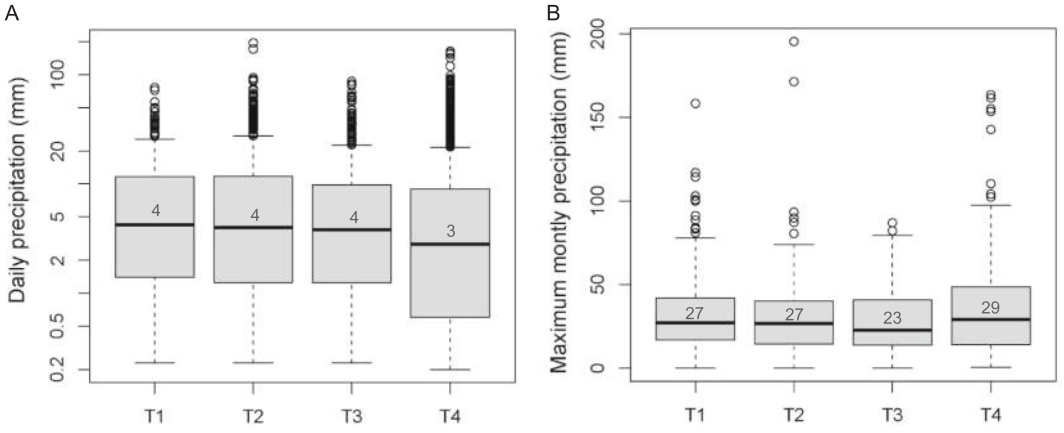



**Fig. 11.** Box and whiskers plots of daily (A) and maximum monthly (B) precipitation. Codes for time periods: T1 = 1954–1975, T2 = 1976–1987, T3 = 1988–1993, T4 = 2001–2019.

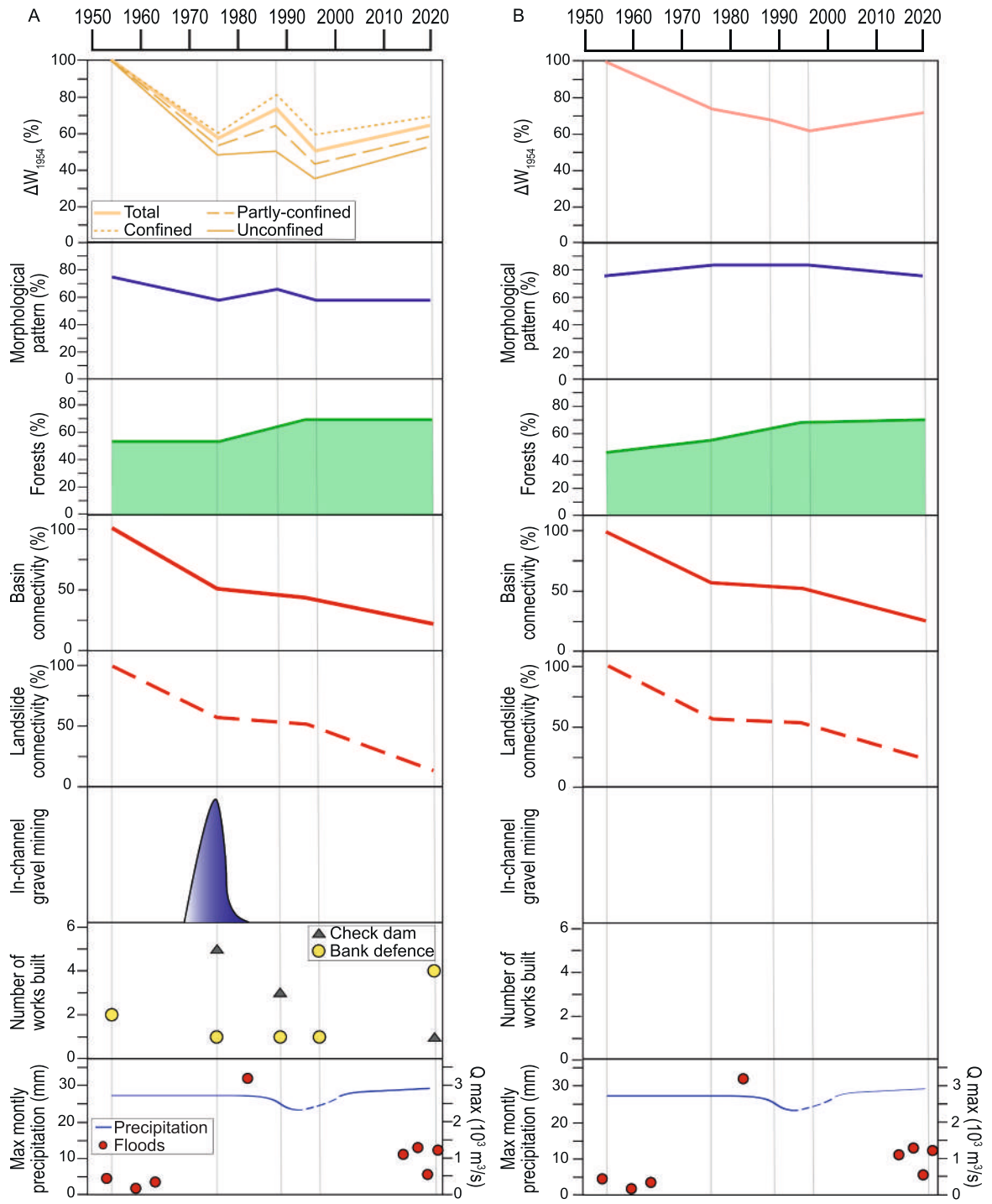



**Fig. 12.** Evolutionary trajectories of the (A) Taro and (B) Ceno rivers in comparison with controlling factors. Morphological pattern refers to reaches with wandering and braided morphology.

in the unconfined reaches; Figs. 4A, C, D, E and 12A). This phase corresponded with a marked pattern simplification, characterized by the emergence of straight morphologies and the reduction of transitional and multi-channel reaches (Figs. 5D and 12A). In contrast, narrowing in the Ceno River was gradual and less intense (median −26 %) and characterized by a general stability of wandering and multi-thread patterns (Figs. 4B, 5E, and 12B).

The active channel widening observed in the Taro in 1988 is probably attributable to the combined effect of the extreme flood event in 1982 (Table 3 and Fig. 12A) and the cessation of the mining activities since the beginning of the 1980s. Indeed, typical flood-induced alterations, such as island degradation and bank erosion (Comiti et al., 2011; Grove et al., 2013; Belletti et al., 2014; Scorpio and Comiti, 2024) were evident in some reaches. Between 1996 and 2020, both rivers displayed a morphological recovery, possibly linked to the increase in rainfall (Fig. 11B) and flood frequency in the post-1996 period (Table 3 and Fig. 12).

An exception is the evolution of reaches 22 and 23 in the Taro River, which showed limited active channel changes, and a stable meandering morphology (Figs. 3A and 4F), explained by the presence of bank defence structures already visible in the 1954 orthophoto.

Differences highlighted in the evolution of the Taro and Ceno rivers

provide important insights to support discussion presented in the following Sections 5.2 and 5.3.

### 5.2. The role of post-1950s hillslopes afforestation on sediment disconnectivity

An increase in forest cover, at the expense of shrubs and agricultural areas, was observed in both catchments (approx. +16 % and +24 % between 1954 and 2020, in the Taro and Ceno basins, respectively, Figs. 7 and 12). The main difference between the two basins lies in the timing of afforestation: it began immediately after 1954 in the Ceno (+9 % in 1976; Fig. 12B), and only after 1976 in the Taro (+1 % in 1976; Fig. 12A). Similar trends are common in many other catchments in Europe and Italy, where the post-Second World War period of emigration, compounded by modern industrial development, resulted in land abandonment of mountain areas and subsequent reforestation (Liébault and Piégay, 2001, 2002; Lach and Wyżga, 2002; Taillefumier and Piégay, 2003; Preciso et al., 2012; Dufour et al., 2015; Buendia et al., 2016; Fortugno et al., 2017; Pittau et al., 2024; Scorpio et al., 2024b). As a consequence of land use changes, structural connectivity also declined over time similarly in both basins (Index of sediment Connectivity: −50 % in the Taro and −44 % in the Ceno basin, between 1954 and 1976; −57 %, in the Taro and −48 % in the Ceno, between 1976 and 1994; −79 % in the Taro and −75 % in the Ceno, between 1994 and 2020; Figs. 8 and 12), resulting in the alteration of sediment transfer pathways and a reduction in sediment supply to the rivers. Simultaneously, landslide-prone areas were gradually stabilized (sediment source area reduced by approximately 60 %; Table 4) and declined in structural connectivity in both catchments, particularly between 1976 and 1994.

The general decrease in sediment connectivity observed in this study aligns with the findings of several studies, confirming that changes in land cover can substantially reduce the potential for sediment transfer from source areas to the fluvial network. Other studies have highlighted how vegetation dynamics and anthropogenic modifications (e.g., terracing or road networks) have influenced sediment dynamics by altering topographic connectivity; in particular, afforestation has been associated with decreases in IC values, indicating a reduction in sediment connectivity (Persichillo et al., 2018; Llena et al., 2019, 2024; Wang et al., 2022; Cheng et al., 2025).

Most of the morphological changes observed in the Ceno River are attributable to the reduction in sediment supply from hillslopes, upland areas, and stabilization of mass wasting processes, as direct human interventions (e.g., gravel mining or in-channel works) were not documented within the active channel during the studied period (Fig. 12B). By contrast, the causal link between channel changes in the Taro River and upland afforestation is not straightforward as by the beginning of the 1970s, numerous anthropogenic activities, primary gravel mining and secondary in-channel works, were already well consolidated (Fig. 12A). In conclusion, the limited channel changes observed in the Ceno River - particularly those that occurred between 1954 and 1976, but also throughout the entire period up to 1996 (median narrowing – 26 % in 1976 and - 38 % in 1996, Fig. 12B) - can be attributed exclusively to basin-scale afforestation, landslide stabilization and consequent decrease in sediment connectivity. In the Taro River, by contrast, additional reach-scale anthropogenic factors (see Section 5.3) contributed alongside upland afforestation, amplifying the channel narrowing, which approached or exceeded −40 % between 1954 and 1976 and reached over −65 % by 1996 (Fig. 12A).

The comparison between the Ceno River and the confined reaches of the Taro suggests potential similarities in the controlling factors acting on the headwater zones of the two catchments - both primarily driven by basin-scale processes.

Finally, it is important to highlight a limitation in the approach used for the analysis of sediment connectivity, consisting of the lack of multi-temporal DTMs and detailed information on anthropogenic structures within the tributaries, which may have acted as barriers, thereby reducing longitudinal connectivity. Nevertheless, based on similarities with other catchments located in the Northern Apennines, it is known that most of the torrent control works were built starting from the 1950s (Surian and Rinaldi, 2003; Preciso et al., 2012; Bollati et al., 2014; Scorpio and Piégay, 2021).

### 5.3. The role of in-channel sediment mining on the degradation of the Taro channel

As explained in Sections 4.1 and 5.1, the Taro River experienced much more intense narrowing compared to the Ceno, between 1954 and 1976. Analyses suggest that these differences were mainly related to the in-channel gravel mining, which was absent in the Ceno River but detected along the whole Taro River in the 1975–1981 period, with a total of official sediment volumes mined ranging between 55,000 and 400,000 $m^3$/year (Clerici et al., 2015). The lack of detailed data on volumes extracted prevented a reliable reach scale estimation of sediment removed. However, the mapping of mining areas allowed us to identify the reaches most affected. Indeed, the results showed that, although mining activity was widespread along the entire length of the Taro River, it was mostly localized in partly-confined (mining area/channel area = 0.03 on average, and 0.05 max) and unconfined sectors (average mining area/channel area = 0.14 on average, and 0.34 max), particularly in reaches 19 and 21 (Fig. 13). The appearance of straight and sinuous morphologies in the Taro, observed since 1976, can be attributed to the combined effect of upland afforestation, in-channel works and gravel mining activities (Fig. 13). Indeed, reaches that experienced greater active channel narrowing were the same as those where gravel extraction was more intense (see reaches from 16 to 21 in Fig. 13).

The impact of in-channel gravel mining observed along the Taro River is consistent with channel changes reported for several other rivers. For instance, extraction of sediments in the Po River basin has been estimated at approximately 12 million $m^3$/year between 1960 and 1980 (Surian and Rinaldi, 2003), while in the Tagliamento River and its tributaries, they exceeded 24 million $m^3$ (Rinaldi et al., 2005). Similarly, gravel removal has been estimated on the order of tens of millions of $m^3$ in the Brenta River (Rinaldi et al., 2005), and around 6.1 million $m^3$ in the Etsch River (Scorpio et al., 2024a). These data, although approximate, highlight the scale at which gravel mining occurred and the significant impact it had on the geomorphological stability of river systems. Indeed, in rivers affected by mining activities, narrowing up to 60–80 % or more (Surian and Rinaldi, 2003; Surian et al., 2009; Brenna et al., 2021; Llena et al., 2023; Scorpio et al., 2024a, 2024b), marked simplification of channel morphology (Surian and Rinaldi, 2003; Rinaldi et al., 2005; Scorpio et al., 2015), and widespread incision of 2–4 m, locally exceeding 10 m, occurred (Rinaldi et al., 2005; Wyżga, 2007; Ziliani and Surian, 2012; Scorpio et al., 2020, 2024b; Brenna et al., 2021; Ferrer-Boix et al., 2023; Llena et al., 2023).

In conclusion, the higher degree of channel adjustments documented in the Taro River, compared to the Ceno River, can be explained with the presence of intensive gravel extraction activities – and locally with some in-channel work – which were completely absent in the Ceno.

### 5.4. Comparison with other catchments in the Northern Apennines

A comparison with other rivers/basins located in the Northern Apennines (Table 5), and characterized by geological and geomorphological settings similar to those of the Taro and Ceno rivers, was performed in order to strengthen the discussion presented in Sections 5.2 and 5.3. In all considered basins (Table 5), forest expansion occurred since the 1920s but mainly after World War II, due to natural reforestation, abandonment of agricultural practices on the hillslopes and modification of farming practices from extensive to intensive. Similarly to the Ceno, in the Borbera and Nure basins, forest cover increased particularly before the 1960s/1970s (from 22 % to 48 % in the Borbera;

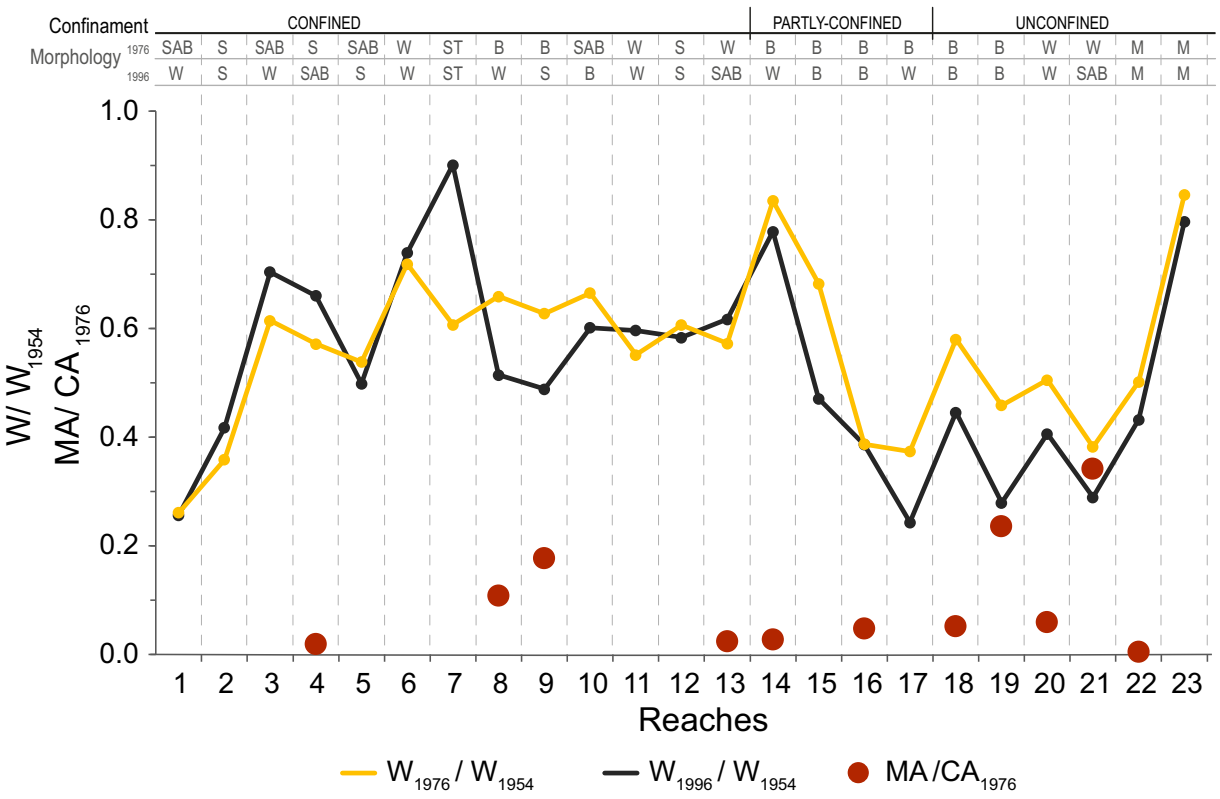



**Fig. 13.** Ratio between: (i) channel width in 1976 and 1954 (yellow line), (ii) channel width in 1996 and 1954 (black line), (iii) mining area (MA) and channel area (CA) in 1976 (red circles). Channel morphology codes, referred to 1976 and 1996: ST = straight; S = sinuous; M = meandering; SAB = sinuous with alternate bars; W = wandering; B = braided.

**Table 5**
Catchment afforestation, human impacts and period of forest cover changes and works construction/activity in the selected rivers of the Northern Apennines.

| River | Catchment scale afforestation | Period of in channel gravel mining | Period of other human works | Reference |
|---|---|---|---|---|
| Nure | 1920s–1970s (+12 %) 1970s- 1990s (+6 %) 1990s- 2012 (+1 %) | 1980s – 1990s | CD since 1977 ICW 1800 – 1990s | Scorpio and Piégay, 2021 |
| Borbera | 1920s–1960s (+26 %) 1960s–1990s (+18) 1990s-2012 (−2 %) | Mid-1980s | CD since 1980s in the main channel CD since 1960s in the tributaries | Scorpio and Piégay, 2021 |
| Trebbia | 1880s–1970s (+15 %) 1970s–1990s (+6 %) 1990s–2000s (+8 %) | After World War II Max rate 1960s - 1980s | D - CD 1950s–1970s ICW 1920s–1980s | Bollati et al., 2014 |
| Parma | 1853–1954 (+6 %) 1954–2007 (+17 %) | 1920s–1990s Max rate 1950s–1980s | CD – ICW 1950s–1990s D 2004 | Brenna et al., 2021 |
| Secchia | Since 1940s | 1960s- 1980s | D 1950s- 1970s ICW | Surian et al., 2009 |
| Panaro | Since 1920s–1930s | 1960s–1990s | ICW 1920s–1960s CD 1970s–1980s D 1950s | Rinaldi et al., 2008; Surian et al., 2009 |

codes: CD = check dam; ICW = in-channel work (groynes, bank protection, levee); D = dam.

from 33 % to 45 % in the Nure), and mainly in the upper part of the catchments (Scorpio and Piégay, 2021). Notably, in the Nure River, an upstream-to-downstream gradient in forest cover increase and in-channel narrowing was observed (Scorpio and Piégay, 2021). In the Trebbia, a progressive increase of forests between 1885 and 2006 (from 22 % to 51 % of the catchment area) is reported by Bollati et al. (2014); while Brenna et al. (2021) - in the Parma basin - describe a significant increase in the area covered by forest, especially from 1954 to 2017 (from 30 % to 47 % of the basin area). Similarly to the Taro River, in the Trebbia, Parma, Secchia and Panaro rivers, intensive gravel mining was carried out after World War II, with peak rates between the 1950s/1960s and the 1980s (see Table 5 for more details), and official values of 3 million $m^3$ of sediments extracted during the twentieth century in the Parma and 5.9 million $m^3$ extracted between 1962 and 1980 in the Panaro. To the contrary, gravel excavation in the Nure and the Borbera rivers started only during the 1980s. Bearing in mind the timing of afforestation and gravel mining activities, some similarities in terms of intensity of channel adjustments can be found between the Ceno (median $W_{1970s}/W_{1954}$ = 0.74) and the Nure and Borbera rivers (median $W_{1970s}/W_{1954}$ = 0.77 and 0.80, respectively) and between the Taro (median $W_{1970s}/W_{1954}$ = 0.57) and the Trebbia and Panaro rivers (median $W_{1970s}/W_{1954}$ = 0.60 and 0.54, respectively), during the period between the 1950s and 1970s (Fig. 14A). In other words, in the rivers where gravel excavation was already underway in the 1970s, as in the case of the Taro River (and Trebbia and Panaro), channel narrowing was more intense than in the rivers where it was absent or started some years/decades later (mid-1980s), as in the case of the Ceno (and Nure and Borbera; Fig. 14A).

By the end of the 1990s, when all rivers had already been affected by gravel mining activities and most in-channel works had been constructed, all channels experienced an acceleration in narrowing (Fig. 14B). Two notable exceptions are the Ceno and the Borbera rivers,

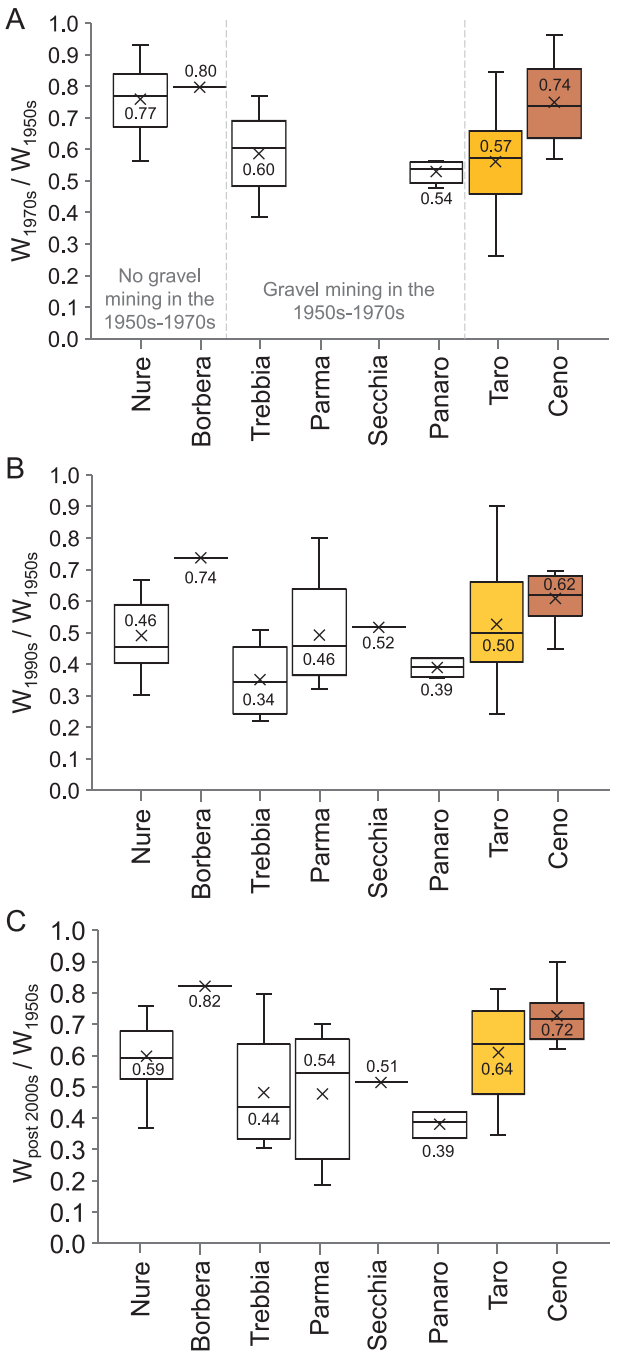



**Fig. 14.** Comparison through box and whiskers plots of: $W_{1970s}/W_{1950s}$ (A), $W_{1990s}/W_{1950s}$ (B), $W_{post2000s}/W_{1950s}$ (C). Data from: Rinaldi et al., 2008; Surian et al., 2009; Bollati et al., 2014; Brenna et al., 2021; Scorpio and Piégay, 2021.

whose channel widths and planform morphologies remained almost constant or experienced only a slight narrowing (Fig. 14B). In the Borbera, even though the gravel mining occurred during the mid-1980s, the channel morphology remained stable because the river flowed through confined or partly confined valleys, with hillslopes frequently affected by gravitational processes connected to the channel and able to provide a continuous sediment supply (Scorpio and Piégay, 2021). After the 1990s, all rivers widened or remained stable (Fig. 14C).

In light of this, the past evolutionary trajectories of the Taro and Ceno rivers were also explained indirectly by examining a set of other similar rivers, which were compared in space and time (*location-for-condition* approach; Belletti et al., 2015; Piégay et al., 2020). Therefore, the application of the *location-for-condition* approach supported the interpretation of results discussed in Sections 5.2 and 5.3.

## 6. Conclusions

The evolutionary trajectories reconstructed for the Taro and Ceno rivers, compared with historical data on the anthropogenic actions at both catchment and channel scales, allowed us to draw reliable interpretations of the complex morphological modifications that affected the two rivers and of the cause-effect relations with human pressures. Even though both rivers experienced active channel narrowing, bed level incision, and simplification of the channel pattern, morphological changes were more pronounced in the Taro River, especially between 1954 and 1976. More specifically, channel degradation in the Taro was amplified by the intense gravel mining – completely absent in the Ceno – which was carried out mainly during the 1970s. Notably, in both catchments, forests increased and sediment source areas (e.g., landslides, badlands) decreased, particularly after the 1970s, leading to a general decrease in structural sediment connectivity and in sediment supply to the two rivers. Therefore, the Taro and Ceno rivers represent an ideal case study to discern and quantify the role of catchment scale factors from the effects of in-channel gravel mining in driving active channel adjustments. Based on the main results, the outcomes of this study strengthen the need to carry out integrated analyses at both catchment and reach scales and emphasizes the relevant role of afforestation, sediment source areas and structural sediment connectivity in the interpretation of active channel changes. At the same time, this study confirms the effects that past gravel mining had on the alteration of sediment dynamics of the active channels that experienced the most intense changes. Conversely, in many other studies (Scorpio et al., 2024b and references therein) generalizations regarding the dominant controlling factors were not possible, as post-1950s channel morphology evolution resulted from cumulative anthropogenic disturbances that occurred simultaneously. In these rivers, the concurrency of all possible hydromorphological stressors made it difficult to derive clear cause–effect relations (Stecca et al., 2019) and simple causal links between channel changes and potential controlling factors were not clearly apparent (Scorpio et al., 2024b).

Finally, the lesson learned from the Taro and Ceno case studies demonstrates that channel dynamics are strongly influenced by processes and stressors acting at both catchment and channel scales. These findings highlight the importance of adopting a catchment-scale perspective in river management, as any anthropogenic alteration within the basin can modify sediment supply and connectivity and, over the long term – some decades – significantly impact channel morphology.

## CRediT authorship contribution statement

**Sharon Pittau:** Writing – original draft, Visualization, Validation, Software, Methodology, Investigation, Formal analysis, Data curation. **Vittoria Scorpio:** Writing – original draft, Validation, Supervision, Software, Methodology, Investigation, Funding acquisition, Formal analysis, Data curation, Conceptualization.

## Declaration of competing interest

The authors declare the following financial interests/personal relationships which may be considered as potential competing interests: Vittoria Scorpio reports financial support was provided by University of Modena and Reggio Emilia. Reports a relationship with that includes:. Has patent pending to. If there are other authors, they declare that they have no known competing financial interests or personal relationships that could have appeared to influence the work reported in this paper.

## Acknowledgements

This research was performed within the framework of the PRIN2022 Project "BAD2BED - BADland morphodynamics assessment and hillslope channel BED coupling in the context of global change", Next Generation EU, Mission 4 Component 1 CUP B53D23007030006. Authors thank Alessandra Cervizzi for supporting some remote sensing data editing, and Marco Cavalli and Stefano Crema for productive discussion.

## Data availability

Data will be made available on request.

## References

AdBPo (Autorità di Bacino Distrettuale del Fiume Po), 1999. Linee generali di assetto idraulico e idrogeologico. Elaborato 3.4: Bacino del Taro (Emilia-Romagna). Progetto di Piano Stralcio per l'Assetto Idrogeologico (PAI), adottato con deliberazione n. 1 dell'11 maggio 1999.

AdBPo (Autorità di Bacino Distrettuale del Fiume Po), 2024. Relazione tecnica: Variante al PAI–Fiume Taro da Bedonia alla confluenza nel fiume Po (DSG_30_2024).

AIPO–Agenzia Interregionale per il fiume Po, 2024. http://geoportale.agenziapo.it/web/index.php/it/rilievi-topografici. (Accessed November 2024).

Arpae - Agenzia prevenzione ambiente energia Emilia-Romagna, 2024. Tabelle climatologiche. https://www.arpae.it/it/temi-ambientali/clima/dati-e-indicatori/tabelle-climatiche. (Accessed November 2024).

Arpae-Agenzia prevenzione ambiente energia Emilia-Romagna, 2024. Annali idrologici. https://www.arpae.it/it/temi-ambientali/meteo/report-meteo/annali-idrologici. (Accessed October 2024).

Batalla, R.J., Gomez, C.M., Kondolf, G.M., 2004. Reservoir-induced hydrological changes in the Ebro River basin (Northeastern Spain). J. Hydrol. 290 (1–2), 117–136. https://doi.org/10.1016/j.jhydrol.2003.12.002.

Belletti, B., Dufour, S., Piégay, H., 2014. Regional assessment of the multi-decadal changes in braided riverscapes following large floods (example of 12 reaches in South East of France). Adv. Geosci. 37, 57–71. https://doi.org/10.5194/adgeo-37-57-2014.

Belletti, B., Dufour, S., Piégay, H., 2015. What is the relative effect of space and time to explain the braided river width and island patterns at a regional scale? River Res. Appl. 31 (1), 1–15.

Blanton, P., Marcus, W., 2009. Railroads, roads and lateral disconnection in the river landscapes of the continental United States. Geomorphology 112, 212–227. https://doi.org/10.1016/j.geomorph.2009.06.0.

Bollati, I.M., Pellegrini, L., Rinaldi, M., Duci, G., Pelfini, M., 2014. Reach-scalemorphological adjustments and stages of channel evolution: the case of the Trebbia River (northern Italy). Geomorphology 221, 176–186. https://doi.org/10.1016/j.geomorph.2014.06.007.

Borselli, L., Cassi, P., Torri, D., 2008. Prolegomena to sediment and flow connectivity in the landscape: a GIS and field numerical assessment. Catena 75, 268–277. https://doi.org/10.1016/j.catena.2008.07.006.

Bracken, L.J., Turnbull, L., Wainwright, J., Bogaart, P., 2015. Sediment connectivity: a framework for understanding sediment transfer at multiple scales. Earth Surf. Process. Landf. 40, 177–188. https://doi.org/10.1002/esp.3635.

Brenna, A., Surian, N., Mao, L., 2021. Alteration of gravel-bed river morphodynamics in response to multiple anthropogenic disturbances: insights from the sediment-starved Parma River (northern Italy). Geomorphology 389, 107845. ISSN 0169-555X. https://doi.org/10.1016/j.geomorph.2021.107845.

Brierley, G.J., Fryirs, K.A., 2005. Geomorphology and River Management: Applications of the River Style Framework. Blackwell, Oxford.

Buendia, C., Bussi, G., Tuset, J., Vericat, D., Sabater, S., Palau, A., Batalla, R.J., 2016. Effects of afforestation on runoff and sediment load in an upland Mediterranean catchment. Sci. Total Environ. 540, 144–157. https://doi.org/10.1016/j.scitotenv.2015.07.005.

Cavalli, M., Trevisani, S., Comiti, F., Marchi, L., 2013. Geomorphometric assessment of spatial sediment connectivity in small Alpine catchments. Geomorphology 188, 31–41. https://doi.org/10.1016/j.geomorph.2012.05.007.

Cavalli, M., Goldin, B., Comiti, F., Brardinoni, F., Marchi, L., 2017. Assessment of erosion and deposition in steep mountain basins by differencing sequential digital terrain models. Geomorphology 291, 4–16. https://doi.org/10.1016/j.geomorph.2016.04.009.

Cavalli, M., Vericat, D., Pereira, P., 2019. Mapping water and sediment connectivity. Sci. Total Environ. 673, 763–767. ISSN 0048-9697. https://doi.org/10.1016/j.scitotenv.2019.04.071.

Cheng, S., Yu, X., Li, Z., Duan, L., Xu, X., Wang, K., 2025. Annual variation in sediment connectivity in karst watersheds of southwest China. CATENA 257, 109173. ISSN 0341-8162. https://doi.org/10.1016/j.catena.2025.109173.

Clerici, A., Perego, S., Chelli, A., Tellini, C., 2015. Morphological changes of the floodplain reach of the Taro River (Northern Italy) in the last two centuries. J. Hydrol. 527, 1106–1122. https://doi.org/10.1016/j.jhydrol.2015.05.063.

Comiti, F., Da Canal, M., Surian, N., Mao, L., Picco, L., Lenzi, M.A., 2011. Channel adjustments and vegetation cover dynamics in a large gravel bed river over the last 200 years. Geomorphology 125, 147–159. https://doi.org/10.1016/j.geomorph.2010.09.011.

Crema, S., Cavalli, M., 2018. SedInConnect: a stand-alone, free and open source tool for the assessment of sediment connectivity. Comput. Geosci. 111, 39–45. https://doi.org/10.1016/j.cageo.2017.10.009.

Cucchiaro, S., Cavalli, M., Vericat, D., Crema, S., Llena, M., Beinat, A., Marchi, L., Cazorzi, F., 2019. Geomorphic effectiveness of check dams in a debris-flow catchment using multi-temporal topographic surveys. Catena 174, 73–83. https://doi.org/10.1016/j.catena.2018.11.004.

Davies, T., Campbell, B., Hall, B., Gomez, C., 2013. Recent behavior and sustainable future management of the Waiho River, Westland, New Zealand. J. Hydrol. 52, 41–56.

De Vincenzo, A., Molino, J.A., Molino, B., Scorpio, V., 2017. Reservoir rehabilitation: the new methodological approach of economic environmental defence. Int. J. Sediment Res. 32, 288–294. Available from: https://doi.org/10.1016/j.ijsrc.2016.05.007.

Dethier, E.N., Renshaw, C.E., Magilligan, F., 2022. Rapid changes to global river suspended sediment flux by humans. Science 376 (6600), 1447–1452. https://doi.org/10.1126/science.abn7980.

Downs, P.W., Piégay, H., 2019. Catchment-scale cumulative impact of human activities on river channels in the late Anthropocene: implications, limitations, prospect. Geomorphology 338, 88–104. https://doi.org/10.1016/j.geomorph.2019.03.021.

Dufour, S., Rinaldi, M., Piégay, H., Michalon, A., 2015. How do river dynamics and human influences affect the landscape pattern of fluvial corridors? Lessons from the Magra River, Central-Northern Italy. Landsc. Urban Plan. 134, 107–118. https://doi.org/10.1016/j.landurbplan.2014.10.007.

Ferrer-Boix, C., Scorpio, V., Martín-Vide, J.P., Núñez-González, F., Mora, F., 2023. Massive incision and outcropping in a former braided river due to mining and training. Geomorphology 436, 108774. https://doi.org/10.1016/j.geomorph.2023.108774.

Fortugno, D., Boix-Fayos, C., Bombino, G., 2017. Adjustments in channel morphology due to land-use changes and check dam installation in mountain torrents of Calabria (southern Italy). Earth Surf. Proc. Land. 42 (14), 2469–2483.

Fryirs, K., Brierley, G.J., 2001. Variability in sediment delivery and storage along river courses in Bega catchment, NSW, Australia: implications for geomorphic river recovery. Geomorphology 38, 237–265. https://doi.org/10.1016/S0169-555X(00)00093-3.

Fryirs, K.A., Brierley, G.J., Preston, N.J., Spencer, J., 2007. Catchment-scale (dis) connectivity in sediment flux in the upper Hunter catchment, New South Wales, Australia. Geomorphology 84 (3), 297–316. https://doi.org/10.1016/j.catena.2006.07.007.

García-Ruiz, J.M., Lana-Renault, N., Beguería, S., Lasanta, T., Regüés, D., Nadal-Romero, E., Serrano-Muela, P., López-Moreno, J.I., Alvera, B., Martí-Bono, C., Alatorre, L.C., 2010. From plot to regional scales: interactions of slope and catchment hydrological and geomorphic processes in the Spanish Pyrenees. Geomorphology 120 (3–4), 248–257. https://doi.org/10.1016/j.geomorph.2010.03.038.

Geoportale Emilia-Romagna, 2024a. https://geoportale.regione.emilia-romagna.it/servizi/servizi-ogc/elenco-capabilities-dei-servizi-wms. (Accessed November 2024).

Geoportale Emilia-Romagna, 2024b. Database uso del suolo. https://geoportale.regione.emilia-romagna.it/approfondimenti/database-uso-del-suolo. (Accessed November 2024).

Geoportale Emilia-Romagna, 2024c. https://geoportale.regione.emilia-romagna.it/catalogo/dati-cartografici/altimetria/layer-2. (Accessed November 2024).

Geoportale Nazionale, 2024. Consultazione WMS. https://gn.mase.gov.it/portale/servizio-di-consultazione-wms. (Accessed November 2024).

Grove, J.R., Croke, J., Thompson, C., 2013. Quantifying different riverbank erosion processes during 852 an extreme flood event. Earth Surf. Process. Landf. 38, 1393–1406. https://doi.org/10.1002/esp.3386.

Hassan, M.A., Church, M., Lisle, T.E., Brardinoni, F., Benda, L., Grant, G.E., 2005. Sediment transport and channel morphology of small, forested streams 1. Jawra J. Am. Water Resour. Assoc. 41 (4), 853–876.

Heckmann, T., Cavalli, M., Cerdan, O., Foerster, S., Javaux, M., Lode, E., Smetanová, A., Vericat, D., Brardinoni, F., 2018. Indices of sediment connectivity: opportunities, challenges and limitations. Earth Sci. Rev. 187, 77–108. https://doi.org/10.1016/j.earscirev.2018.08.004.

Hooke, J.M., 2006. Human impacts on fluvial systems in the Mediterranean region. Geomorphology 79 (3–4), 311–335. https://doi.org/10.1016/j.geomorph.2006.06.036.

Kondolf, G.M., 1997. Hungry water: effects of dams and gravel mining. Environ. Manag. 21, 533–551.

Koreňová, S., Michalková, M.Š., Máčka, Z., Pöppl, R., Donoval, J., 2024. Linking sediment connectivity with sediment transport risk assessment in small forested catchments in the Czech Republic. River Res. Appl. https://doi.org/10.1002/rra.4295.

Lach, J., Wyżga, B., 2002. Channel incision and flow increase of the upper Wisłoka River, southern Poland, subsequent to the reafforestation of its catchment. Earth Surf. Process. Landf. 27, 445–462.

Liébault, F., Piégay, H., 2001. Assessment of channel changes due to long term bedload supply decrease, Roubion River, France. Geomorphology 36 (3–4), 167–186. https://doi.org/10.1016/S0169-555X(00)00044-1.

Liébault, F., Piégay, H., 2002. Causes of 20th century channel narrowing in mountain and piedmont rivers of southeastern France. Earth Surf. Process. Landf. 27, 425–444. https://doi.org/10.1002/esp.328.

Liébault, F., Gomez, B., Page, M., Marden, M., Peacock, D., Richard, D., Trotter, C.M., 2005. Land-use change, sediment production and channel response in upland regions. River Res. Appl. 21, 1–18. https://doi.org/10.1002/rra.880.

Llena, M., Vericat, D., Cavalli, M., Crema, S., Smith, M.W., 2019. The effects of land use and topographic changes on sediment connectivity in mountain catchments. Sci.

Total Environ. 660, 899–912. ISSN 0048-9697. https://doi.org/10.1016/j.scitotenv.2018.12.479.
Llena, M., Vericat, D., Martínez-Casasnovas, J.A., Smith, M.W., 2020. Geomorphic adjustments to multi-scale disturbances in a mountain river: a century of observations. CATENA 192, 104584. ISSN 0341-8162. https://doi.org/10.1016/j.catena.2020.104584.
Llena, M., Simonelli, T., Brardinoni, F., 2023. Inherited anthropogenic disturbance and decadal sediment dynamics in a mountain fluvial system: the case of the Marecchia River canyon, Northern Apennines. GSA Bull. 136 (1–2), 741–764. https://doi.org/10.1130/B36720.1.
Llena, M., Nadal-Romero, E., Zabalza-Martínez, J., Cortijos-López, M., Lasanta, T., 2024. Effects of post-abandonment management on surface runoff in a Mediterranean mid-mountain basin. Catena 237, 107775. https://doi.org/10.1016/j.catena.2023.107775.
Marchi, L., Comiti, F., Crema, S., Cavalli, M., 2019. Channel control works and sediment connectivity in the European Alps. Sci. Total Environ. 668, 389–399. https://doi.org/10.1016/j.scitotenv.2019.02.416.
Najafi, S., Dragovich, D., Heckmann, T., Sadeghi, S.H., 2021. Sediment connectivity concepts and approaches. Catena 196, 104880. https://doi.org/10.1016/j.catena.2020.104880.
Persichillo, M.G., Bordoni, M., Cavalli, M., Crema, S., Meisina, C., 2018. The role of human activities on sediment connectivity of shallow landslides. Catena 160, 261–274. https://doi.org/10.1016/j.catena.2017.09.025.
Piasecka, J., Święchowicz, J., Najwer, A., Zwoliński, Z., 2025. Impact of the water reservoir and river engineering structures on longitudinal and transverse (Dis) connectivity associated with sediment transfer. Land Degrad. Dev. 36 (8), 2609–2638. https://doi.org/10.1002/ldr.5519.
Piégay, H., Arnaud, F., Belletti, B., Bertrand, M., Bizzi, S., Carbonneau, P., Dufour, S., Liébault, F., Ruiz-Villanueva, V., Slater, L., 2020. Remotely sensed rivers in the Anthropocene: state of the art and prospects. Earth Surf. Process. Landforms 45, 157–188. https://doi.org/10.1002/esp.4787.
Pitscheider, F., Steger, S., Cavalli, M., Comiti, F., Scorpio, V., 2024. Areas simultaneously susceptible and (dis-)connected to debris flows in the Dolomites (Italy): regional scale application of a novel data-driven approach. J. Maps 20 (1), 1–14. https://doi.org/10.1080/17445647.2024.2307549.
Pittau, S., Rossi, M., Llena, M., Brardinoni, F., 2024. Evaluating historical, basin-wide landslide activity in a context of land abandonment and climate change: effects of landslide visibility and temporal resolution. Geomorphology 452, 109122. ISSN 0169-555X. https://doi.org/10.1016/j.geomorph.2024.109122.
Poeppl, R.E., Keesstra, S.D., Maroulis, J., 2017. A conceptual connectivity framework for understanding geomorphic change in human-impacted fluvial systems. Geomorphology 277, 237–250. https://doi.org/10.1016/j.geomorph.2016.07.033.
Poeppl, R.E., Fryirs, K.A., Tunnicliffe, J., Brierley, G.J., 2020. Managing sediment (dis) connectivity in fluvial systems. Sci. Total Environ. 736, 139627. https://doi.org/10.1016/j.scitotenv.2020.139627.
Preciso, E., Salemi, E., Billi, P., 2012. Land use changes, torrent control works and sediment mining: effects on channel morphology and sediment flux, case study of the Reno River (Northern Italy). Hydrol. Process. 26 (8), 1134–1148. https://doi.org/10.1002/hyp.8202.
R Core Team, 2020. R: A Language and Environment for Statistical Computing. R Foundation for Statistical Computing. https://www.Rproject.org.
Reid, L.M., Dunne, T., 1996. Rapid Evaluation of Sediment Budgets. Catena Verlag, Reiskirchen, Germany.
Rinaldi, M., Simon, A., 1998. Bed-level adjustments in the Arno River, Central Italy. Geomorphology 22, 57–71.
Rinaldi, M., Wyzga, B., Surian, N., 2005. Sediment mining in alluvial channels: physical effects and management perspectives. River Res. Appl. 21 (7), 805–828. https://doi.org/10.1002/rra.884.
Rinaldi, M., Teruggi, L., Simoncini, C., Nardi, L., 2008. Dinamica recente ed attuale di alvei fluviali: alcuni casi di studio appenninici (Italia centro-settentrionale). Alpine Mediterr. Quat. 21 (1B), 291–302. https://amq.aiqua.it/index.php/amq/article/view/362.
Rollet, A.J., Piégay, H., Dufour, S., Bornette, G., Persat, H., 2014. Assessment of consequences of sediment deficit on a gravel river bed downstream of dams in restoration perspectives: application of a multicriteria, hierarchical and spatially explicit diagnosis. River Res. Appl. 30 (8), 939–953. https://doi.org/10.1002/rra.2689.
Scorpio, V., Comiti, F., 2024. Channel changes during and after extreme floods in two catchments of the Northern Apennines (Italy). Geomorphology 463, 109355. ISSN 0169-555X. https://doi.org/10.1016/j.geomorph.2024.109355.
Scorpio, V., Piégay, H., 2021. Is afforestation a driver of change in Italian rivers within the Anthropocene era? Catena 198, 105031. https://doi.org/10.1016/j.catena.2020.105031.
Scorpio, V., Aucelli, P.P.C., Giano, I., Pisano, L., Robustelli, G., Rosskopf, C.M., Schiattarella, M., 2015. River channel adjustment in Southern Italy over the past 150 years and implications for channel recovery. Geomorphology 251, 77–90. https://doi.org/10.1016/j.geomorph.2015.07.008.
Scorpio, V., Zen, S., Bertoldi, W., Surian, N., Mastronunzio, M., Dai Prá, E., Zolezzi, G., Comiti, F., 2018. Channelization of a large Alpine River: what is left of its original morphodynamics? Earth Surf. Process. Landforms 43 (5), 1044–1062. Available from: https://doi.org/10.1002/esp.4303.
Scorpio, V., Andreoli, A., Zaramella, M., Moritsch, S., Theule, J., Dell' Agnese, A., Muhar, S., Borga, M., Bertoldi, W., Comiti, F., 2020. Restoring a glacier-fed river: past and present morphodynamics of a degraded channel in the Italian Alps. Earth Surf. Process. Landforms 45, 2804–2823. https://doi.org/10.1002/esp.4931.
Scorpio, V., Cavalli, M., Steger, S., Crema, S., Marra, F., Zaramella, M., Borga, M., Marchi, L., Comiti, F., 2022. Storm characteristics dictates sediment dynamic and geomorphic changes in mountain channels: a case study in the Italian Alps. Geomorphology 403, 108173. https://doi.org/10.1016/j.geomorph.2022.108173.
Scorpio, V., Andreoli, A., Dinkelaker, N., Marchese, E., Coviello, V., Gems, B., Vignoli, G., Comiti, F., 2024a. Multi-decadal quantification of interactions between coarse sediment fluxes and channel management in South Tyrol, Eastern European Alps. Earth Surf. Process. Landf. 1–21. https://doi.org/10.1002/esp.5804.
Scorpio, V., Comiti, F., Liébault, F., Piégay, H., Rinaldi, M., Surian, N., 2024b. Channel changes over the last 200 years: a meta data analysis on European rivers. Earth Surf. Process. Landf. 49 (9), 2651–2676. https://doi.org/10.1002/esp.5848.
Stecca, G., Zolezzi, G., Murray Hicks, D., Surian, N., 2019. Reduced braiding of rivers in human-modified landscapes: converging trajectories and diversity of causes. Earth Sci. Rev. 188, 291–311. https://doi.org/10.1016/j.earscirev.2018.10.016.
Surian, N., 2022. Fluvial changes in the anthropocene: a European perspective. In: Shroder, J.J.F. (Ed.), Treatise on Geomorphology, vol. 9. Elsevier, Academic Press, pp. 561–583. https://doi.org/10.1016/B978-0-12-818234-5.00109-7.
Surian, N., Rinaldi, M., 2003. Morphological response to river engineering and management in alluvial channels in Italy. Geomorphology 50 (4), 307–326. https://doi.org/10.1016/S0169-555X(02)00219-2.
Surian, N., Ziliani, L., Comiti, F., Lenzi, M.A., Mao, L., 2009. Channel adjustments and alteration of sediment fluxes in gravel-bed rivers of North-Eastern Italy: potentials and limitations for channel recovery. River Res. Appl. 25, 551–567. https://doi.org/10.1002/rra.1231.
Taillefumier, F., Piégay, H., 2003. Contemporary land use change in prealpine Mediterranean mountains: a multivariate GIS-based approach to two municipalities in the Southern French Alps. Catena 51, 267–296. https://doi.org/10.1016/S0341-8162(02)00168-6.
Thorne, C.R., 1997. Channel types and morphological classification. In: Thorne, C.R., Hey, R.D., Newson, M.D. (Eds.), Applied Fluvial Geomorphology for River Engineering and Management. Wiley, pp. 175–222.
Tischendorf, L., Fahrig, L., 2000. How should we measure landscape connectivity? Landsc. Ecol. 15 (7), 633–641. https://doi.org/10.1023/A:1008177324187.
Vergari, F., Troiani, F., Cavalli, M., Faulkner, H., Del Monte, M., 2025. Shifts in hillslope-channel connectivity after land reclamation in a Mediterranean semi-humid badland landscape. CATENA 254, 108921. ISSN 0341-8162. https://doi.org/10.1016/j.catena.2025.108921.
Wainwright, J., Turnbull, L., Ibrahim, T.G., Lexartza-Artza, I., Thornton, S.F., Brazier, R.E., 2011. Linking environmental régimes, space and time: interpretations of structural and functional connectivity. Geomorphology 126, 387–404.
Wang, C.S., Zhang, G.H., Zhu, P.Z., Wang, Z.G., Xing, S.K., 2022. Sediment connectivity of small watershed affected by gully development and vegetation restoration on the loess plateau. Geoderma 410, 115663. https://doi.org/10.1016/j.geoderma.2021.115663.
Wohl, E., 2006. Human impacts to mountain streams. Geomorphology 79 (3–4), 217–248. https://doi.org/10.1016/j.geomorph.2006.06.020.
Wohl, E., 2020. Rivers in the Anthropocene: the U.S. perspective. Geomorphology 366, 106600. https://doi.org/10.1016/j.geomorph.2018.12.001.
Wohl, E., Brierley, G., Cadol, D., Coulthard, T.J., Covino, T., Fryirs, K.A., Grant, G., Hilton, R.G., Lane, S.N., Magilligan, F.J., Meitzen, K.M., Passalacqua, P., Poeppl, R.E., Rathburn, S.L., Sklar, L.S., 2019. Connectivity as an emergent property of geomorphic systems. Earth Surf. Process. Landforms 44, 4–26. https://doi.org/10.1002/esp.4434.
Wyżga, B., 2007. A review on channel incision in the Polish Carpathian rivers during the 20th century. Dev. Earth Surf. Process. 11, 525–553.
Zawiejska, J., Wyżga, B., 2010. Twentieth-century channel change on the Dunajec River, southern Poland: patterns, causes and controls. Geomorphology 117, 234–246.
Ziliani, L., Surian, N., 2012. Evolutionary trajectory of channel morphology and controlling factors in a large gravel-bed river. Geomorphology 173–174, 104–117. https://doi.org/10.1016/j.geomorph.2012.06.001.